RARE EARTH BORIDES:
THE SAMARIUM-BORON SYSTEM

Thesis for the Degree of Ph. D.
MICHIGAN STATE UNIVERSITY
George Dennis Sturgeon
1964

THESIS
C. 2

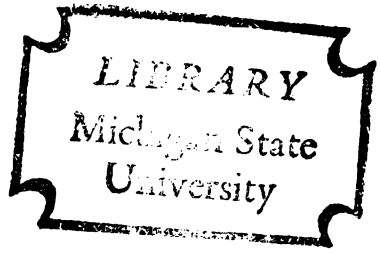

MICHIGAN STATE UNIVERSITY
DEPARTMENT OF CHEMISTRY
EAST LANSING, MICHIGAN

RARE EARTH BORIDES: THE SAMARIUM-BORON SYSTEM

By

George Dennis Sturgeon

A THESIS

Submitted to
Michigan State University
in partial fulfillment of the requirements
for the degree of

DOCTOR OF PHILOSOPHY

Department of Chemistry

1964

B35849

ACKNOWLEDGMENTS

The author is very pleased to acknowledge the guidance of Dr. Harry A. Eick and to thank Dr. Gordon L. Galloway and Mr. Paul Nordine for their illuminating comments and personal interest during the course of this research.

The financial assistance provided by the Atomic Energy Commission has been very welcome.

Finally, the author would like to take this opportunity to express his deep appreciation to the multitude of people who, willingly or unwittingly, have had a hand in making this thesis a reality.

TABLE OF CONTENTS

TABLE OF CONTENTS (Cont.)

LIST OF TABLES

LIST OF FIGURES

LIST OF APPENDICES

I. INTRODUCTION

Rare earth borides are not thoroughly characterized physically or chemically, but recent years have witnessed a large increase in knowledge of these borides, particularly with regard to the preparation of previously unknown compounds.

The specific interest in materials for high temperature applications together with the unusual electrical and thermal properties exhibited by many binary metal borides have been the primary forces behind much of the research in this fertile area. But the properties of binary borides: high melting points, high boiling points, hardness, inertness and the difficulty of classifying these borides in terms of chemical and metallurgical bonding rules, compounded by the problems confronted in conducting research in this area are sufficient to arouse the interest of the scientist.

While it is generally true that the properties of the rare earths and their compounds are uniquely similar, the student of rare earth chemistry is concerned primarily with the differences in the behavior of these metals. The common educational practice of considering the rare earths as an isolated group among the elements seems to have resulted in a dearth of attention to the problem of relating and unifying the properties of the lanthanons with the properties of the metals lying outside this classification.

In the case of the rare earth borides, the relationship between these and the borides of the outer transition metals is compounded by the fact that the rare earth metals and the outer transition metals

exhibit borides of quite divergent stoichiometries with relatively few instances of the same stoichiometry and structure appearing for borides of both groups of metals. For example, typical stoichiometries of the transition metals are M_4B, M_3B, M_7B_3, M_2B, $M_{11}B_8$, M_5B_3, M_3B_2, M_4B_3, MB, M_3B_4, M_2B_3, MB_2, M_2B_5 and MB_3, whereas typical stoichiometries of the rare earth borides are MB_x where x is 2, 4, 6, or 12.

The difficulty in obtaining pure samples of the rare earth metals and their compounds, long a barrier to rapid and substantial progress in rare earth chemistry now largely has been removed. At the present time, the problems confronting the chemist dealing with binary rare earth compounds are very frequently those of high temperature technology, i.e. achieving, controlling and measuring high temperatures, containing reactive mixtures at high temperatures and determining one or more properties of such systems.

The importance of the element boron in any discussion of borides can hardly be over-stated. It is time that the interest in the heavy metal* in binary borides be balanced with corresponding emphasis on boron's contribution to the chemistry of these compounds. Boron which is positioned on the edge of the metallic elements of the periodic table, has properties which make it fascinating and at times unique. Foremost among these properties are the propensity of boron atoms to form bonds with other boron atoms whenever possible, the ability to form five or

*It would be tedious to preceed the word "metal" with the adjective "heavy" when referring to the non-boron member of binary borides. Therefore the word "metal" will be used alone unless clarity demands further specification.

more bonds per boron atom even though boron is in the first eight-member period of the table of elements, and the striking rigidity of three dimensional boron structures such as are found in many binary borides.

A. Literature Concerning Rare Earth Borides

The literature on binary rare earth borides, firmly rooted in the work of Andrieux (1), Allard (2) and of von Neuman and Stackleberg (3), only recently has begun to expand. The publication of several review papers and compilations of crystallographic data (4-9) have been of great benefit to workers in the area. Unfortunately, the literature has not been so exclusive as to prevent the appearance of suspect and unsubstantiated reports.

The list of borides of the lanthanons is being lengthened almost constantly as reports of new compounds appear (7-28). Such reports generally contain information concerning the preparative method, the rough stoichiometry of the product boride and X-ray powder diffractometry data demonstrating the structure.

B. The Structures of the Rare Earth Borides

It should be noted immediately that, in general, X-ray data provide only information concerning the arrangement of the metal atoms so that the positions of the boron atoms in a unit cell must be assigned on the basis of symmetry and geometric arguments.

The diborides of the rare earths are of simple structure with hexagonal unit cells of space groups P6/mmm with one formula weight per unit cell. The metal atom is at the origin of the unit cell (0,0,0)

with the boron atom positions at (1/3,2/3,1/2) and (2/3,1/3,1/2) (Fig. 1). The metal and boron atoms thus occupy alternate planes with the boron atoms forming hexagonal networks in the (0,0,1/2) plane.

The cubic hexaborides have a cesium chloride type lattice of space group Pm3m with one formula unit per unit cell. The metal atom may be considered to be located at the center of the cell (1/2,1/2,1/2) with the boron atoms located at (± x,0,0), (0,±x,0) and (0,0,±x) (Fig. 2). The only variable position parameter, x, has not been determined because of the difficulties associated with the location of light atoms in the presence of heavier atoms. Generally the boron atoms are considered to form octahedral groups centered on the point (0,0,0) with each of the six boron atoms at one of the vertices of the octahedron. The boron positions are easily established by simple geometric considerations if all boron-boron bond distances are assumed to be equal. The validity of this assumption can be ascertained only by very precise X-ray diffraction studies.

The tetraborides are tetragonal containing four formula units per unit cell; the space group is P4/mbm. The metal atoms are arranged in planes, each metal having five iso-elemental neighbors. In the spaces between metal atoms, the boron atoms are arranged in planar groups where the boron atoms have an arrangement much like that of the diborides or in octahedral groups much like those of the hexaborides (Fig. 3). The boron atoms of either type are in contact and form a continuous three-dimensional network, but with the majority of the atoms in the z = 1/2 plane. Thus, the tetraborides may be viewed as hybrids of the diborides and hexaborides in terms of structure as well as stoichiometry.

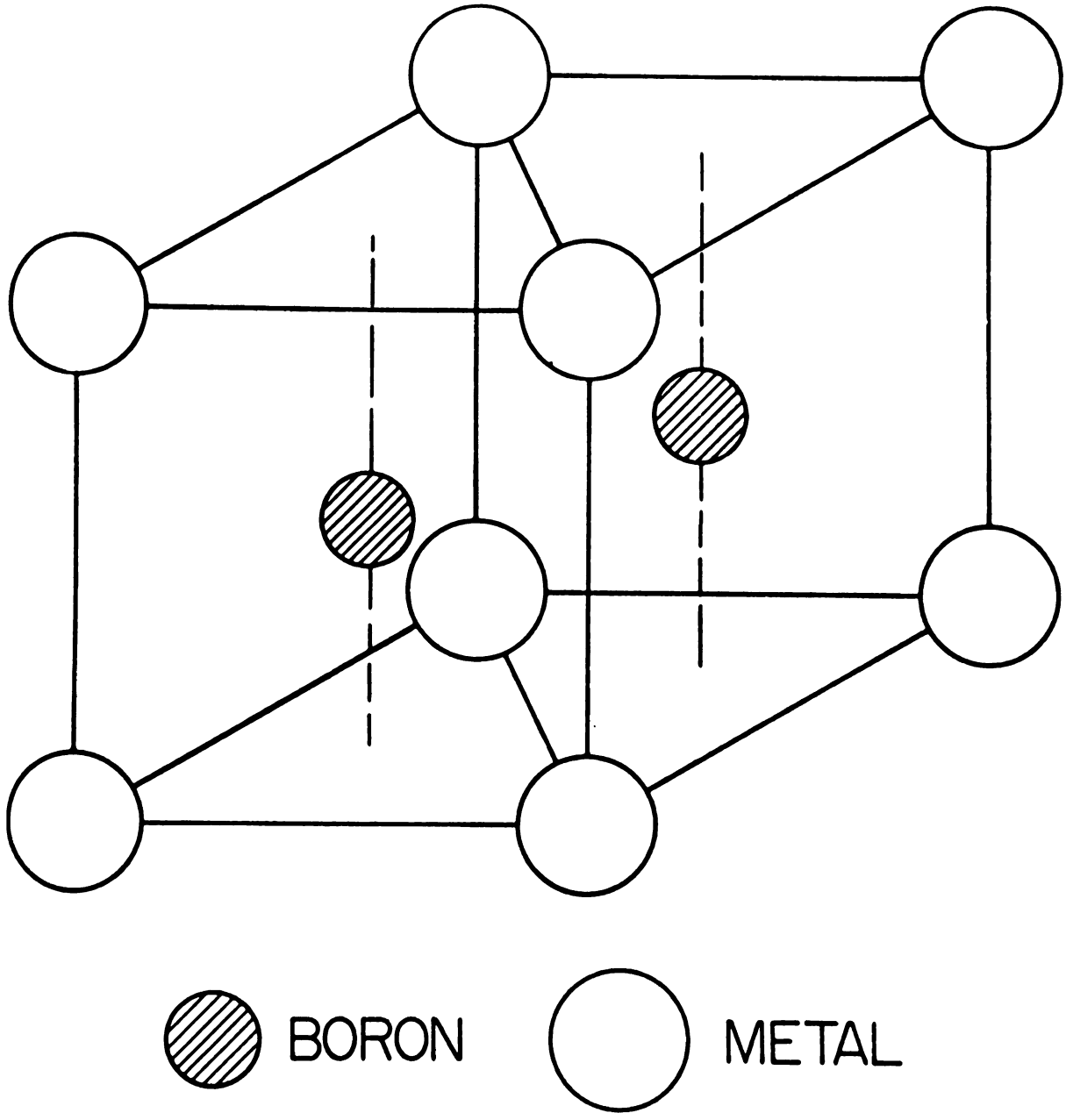

Figure 1a (9). The unit cell structure of binary metal diborides.

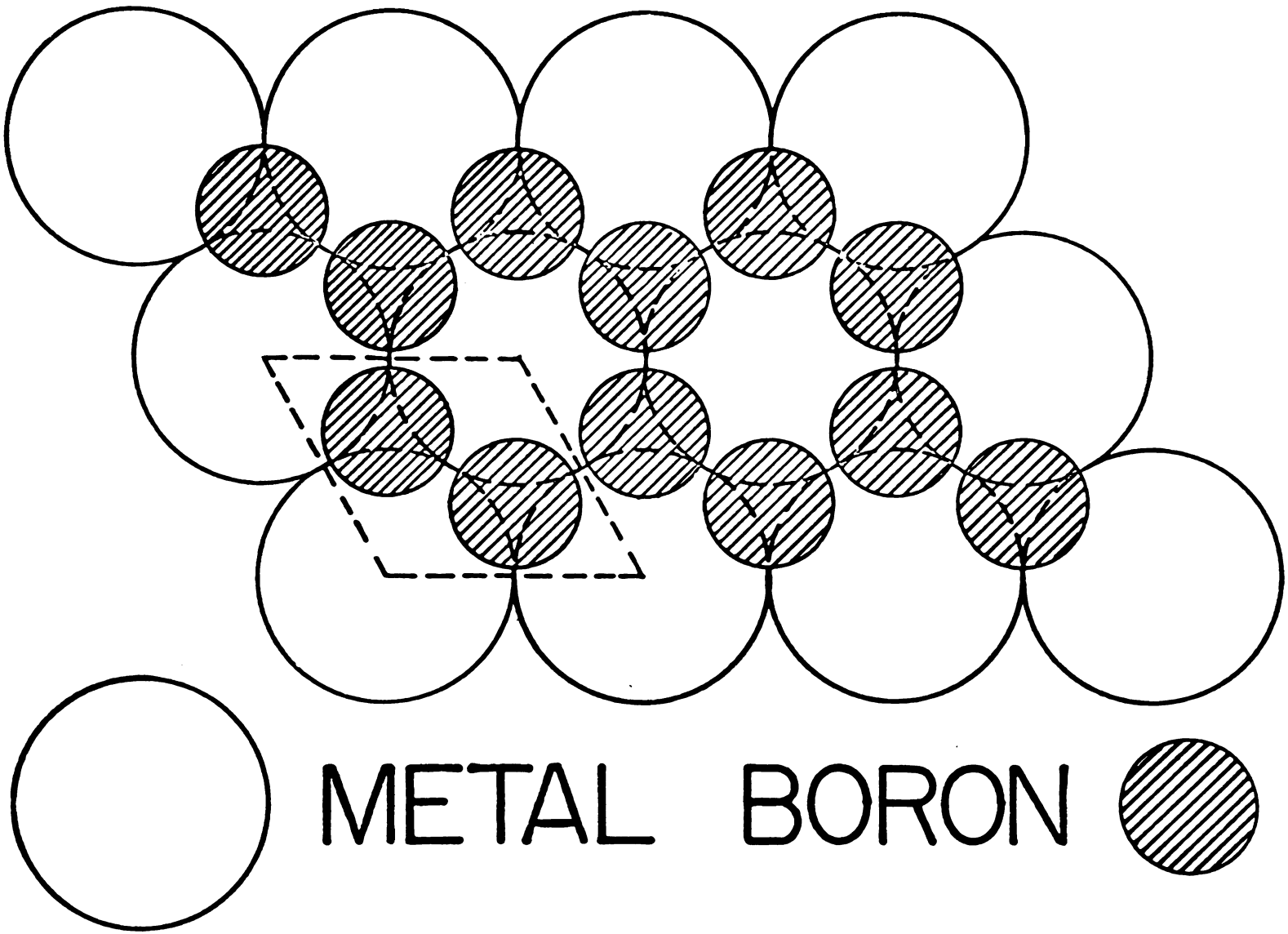

Figure 1b (9). The structure of binary metal diborides showing alternate layers of boron and metal atoms.

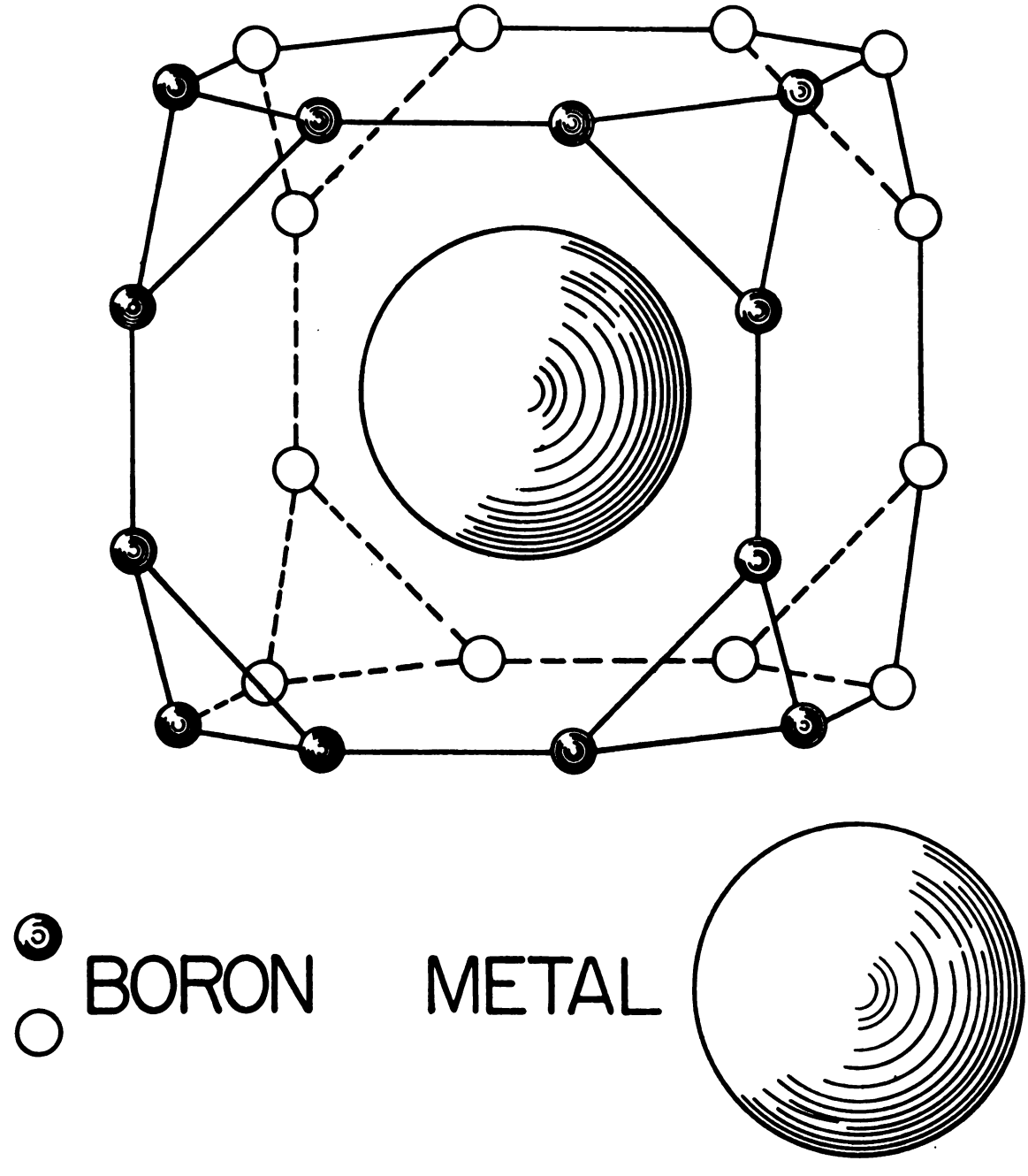

Figure 2a (9). The boron environment of the central metal in cubic hexaborides.

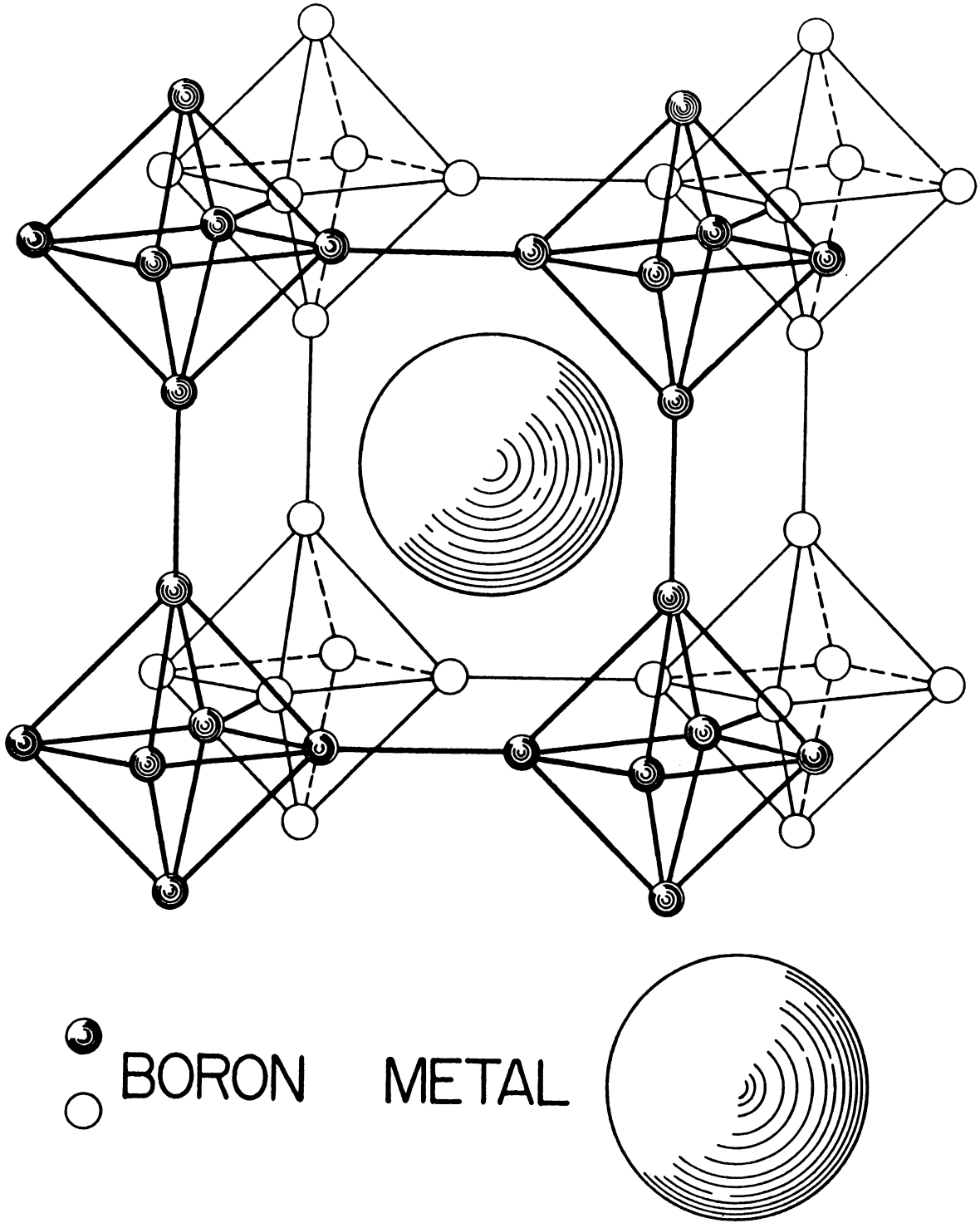

Figure 2b (9). The structure of the cubic hexaborides showing the boron lattice.

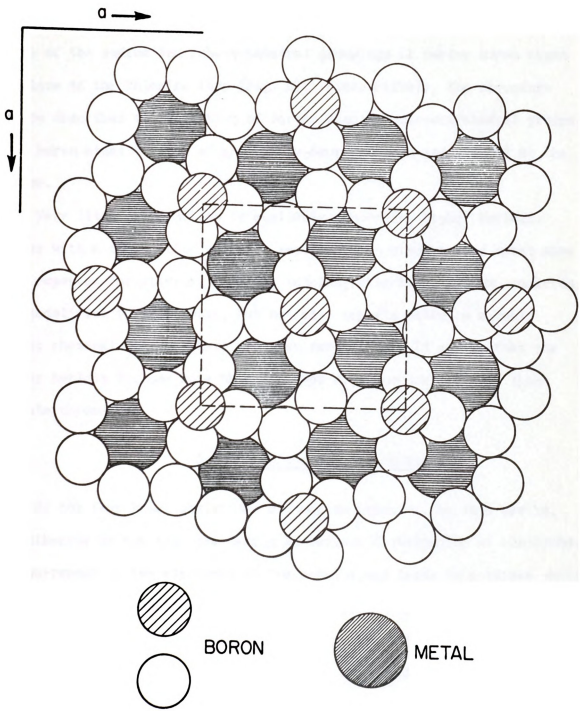

Figure 3 (9). The structure of the metal tetraborides; projection of the structure on the (001) plane.

The dodecaborides are also cubic of space group Fm3m with four formula units per unit cell. The structure may be visualized in terms of a modified sodium chloride type structure with the metal atoms in place of the sodium and cubo-octahedral groupings of twelve boron atoms in place of the chloride ions (Fig. 4). Alternatively, the structure can be described as consisting of larger regular cubo-octrahedral groups with boron atoms at each of the twenty-four vertices and a metal at the center.

Very little information is available concerning higher borides. Phases with a composition of about seventy boron atoms to one metal have been reported for yttrium, holmium, terbium, ytterbium, erbium, samarium, and gadolinium (9,28). Most, but not all, reports refer to a cubic phase; chemical analyses have not been definitive. It may be that the higher borides include more than one type of structure and more than one stoichiometry.

C. Bonding in the Rare Earth Borides

Of the four known stoichiometric boride types of the rare earths, the diboride is the only one having an obvious distribution of electrons. The surrender of two electrons by the metal atoms leads to a closed shell structure, the borons having gained enough electrons to possess a graphitic electronic structure as well as graphitic geometry. It is more surprising to find that the best available calculations and experimental data indicate that the metal atom is required to donate two and no more electrons to the boron lattice no matter which boride is involved (29-33).

Because the hexaborides are most familiar and because quantum mechanical calculations are simplest for a cubic structure, the hexaborides

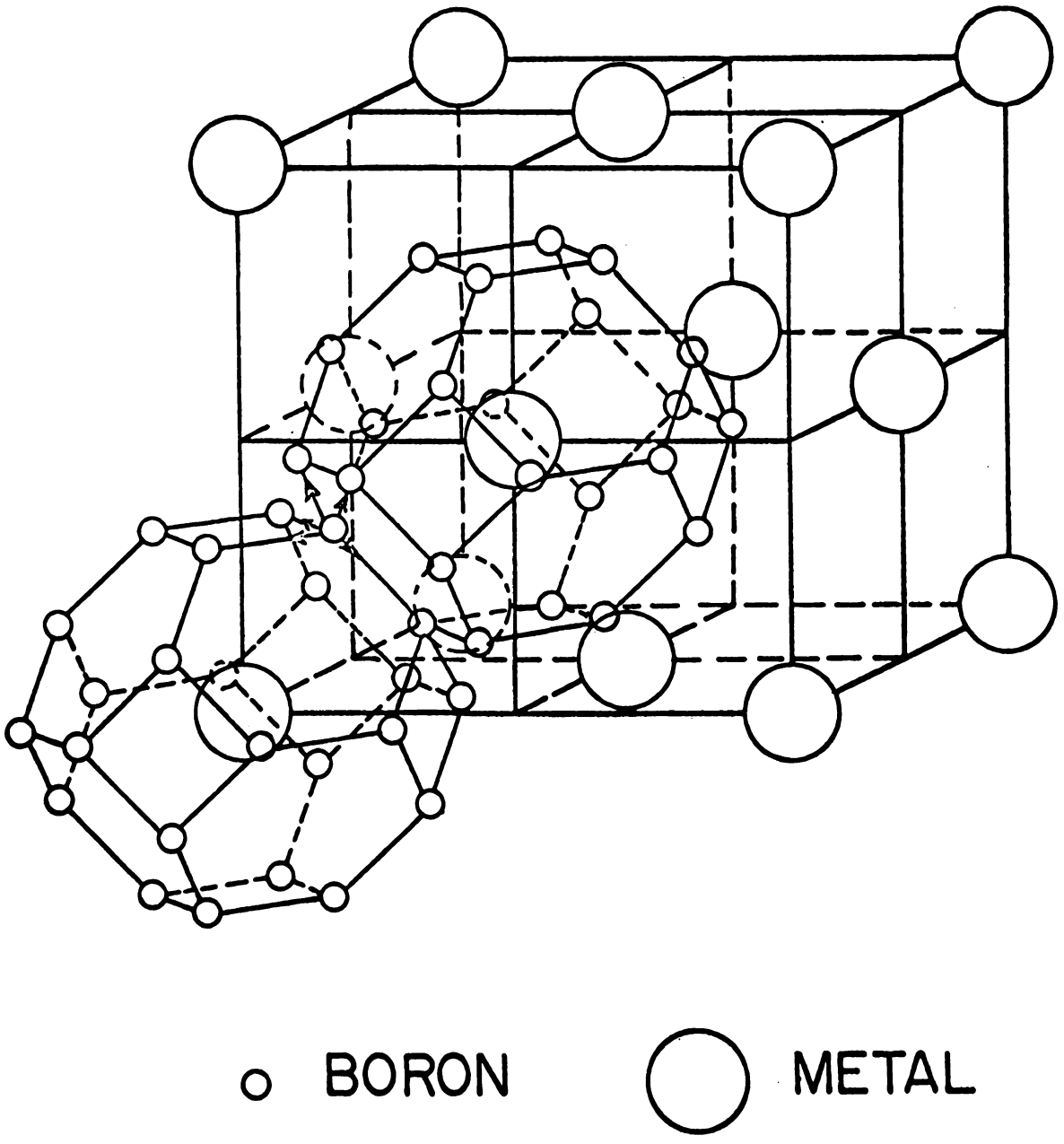

Figure 4b (9). The structure of the binary dodecaborides showing the boron lattice.

have been studied more thoroughly than any of the other borides. Several separate discussions of the bonding in the hexaborides have concentrated on the internal orbitals of the B_6 octahedral group with six external bonds to other, like octahedra. The electron requirement is the sum of the six electrons used for the external orbitals and seven pairs of electrons used for internal bonding orbitals amounting to twenty electrons per octahedron. Hence, two electrons must be provided by the metal since the six boron atoms supply eighteen.*

Lipscomb and Britton (33) have studied the electron requirements of the boron atom groupings in the tetraboride unit cell which includes four metal atoms and sixteen boron atoms. Twelve of the boron atoms are members of octahedra like those in the hexaborides. Since each octahedron requires twenty electrons to fill the orbitals of its external and internal bonds, a total of forty electrons are needed for the boron octahedra. The other four boron atoms are grouped into two pairs joined internally by an ethylenic bond which requires four electrons per pair or eight electrons. In addition, each boron atom in the ethylenic group is joined externally to two other boron atoms (which are part of octahedra) by single bonds for which one electron is needed. The four such boron atoms with two single bonds each therefore require eight electrons for external orbitals. Of the sum of fifty-six electrons (forty plus eight plus eight) required, the boron atoms themselves

*There is evidence that the B_6 group does not require a full two electrons from the metal since a Group I metal, sodium, has been substituted for the Group II metal calcium in its hexaboride to the extent that only 1.6 electrons are statistically available to each B_6 group (11).

provide forty-eight so that each of the four metal atoms in the unit cell must supply two electrons to make up the eight additional electrons.

Lipscomb and Britton also have used an LCAO molecular orbital approach to calculate the electron requirements for dodecaborides; the cubo-octahedra require twenty-six electrons for internal orbitals and one electron for each of the twelve boron atoms for a single bond to a like boron in an adjacent cubo-octahedron. Of the total of thirty eight electrons required (twenty-six plus twelve), thirty-six are available from the twelve boron atoms themselves leaving a deficiency of two electrons to be made up by the metal atom.

These models previously suffered from a lack of experimental substantiation. However, experimental data reported by Johnson and Daane (34,35) support these models. On the basis of electrical conductivity and Hall Effect measurements on CaB_6, SrB_6, BaB_6, YB_2, YB_4, YB_6, and YB_{12} they report results which are in agreement with the models invoked above. Thus the alkaline earth borides were found to be semiconductors while the yttrium di-, hexa- and dodecaborides were found to have one free electron per yttrium atom in each compound. In the case of the tetraboride, it was impossible to obtain a calculated value for the Hall coefficient to compare with the experimentally determined value, but the measured value does not contradict the model discussed above, and the electron requirements of the octahedral boron units in the tetraborides have been established from the work on hexaborides.

D. The Specific Purpose of This Research

The state of knowledge of rare earth borides was summarized by Eick in a paper presented at a seminar at Lake Arrowhead, California in October 1960 and subsequently published as a chapter in the book Rare Earth Research (8). Because of the very limited amount of data more than qualitative in nature, some speculations and tentative conclusions were drawn from the information then available.

In Eick's discussion of the rare earth hexaborides appear the following comments:

> Although the lattice parameters of lutetium, thulium, and erbium hexaborides are probably in error by a small amount, it is readily noticeable that they do not decrease in size proportionally to the other members (of the series of rare earth hexaborides). This very small decrease may indicate that the boride lattice can contract no further and the smaller metal atoms are simply held, as it were, rather loosely in a boron cage. Other non-rare earth hexaborides have larger lattice parameters.

and "..... ErB_6 may not be prepared readily because of the instability of ErB_6 with respect to ErB_4 and boron at the temperatures necessary for the reaction (of Er_2O_3 with elemental boron)."

In work reported in another place, Eick and Gilles (36) determined precise lattice parameters of some rare earth borides. In that work, the smallest rare earth metal for which a hexaboride could be prepared was holmium.

Two important observations were thus gleaned: that formation of rare earth hexaborides becomes progressively more difficult to induce as the metallic radius of the metal involved becomes smaller and that the lattice parameters reported for the hexaborides of erbium, thulium and lutetium are not entirely consistent with those of the other rare earth hexaborides.

In the face of continuing reports emanating from the Soviet Union (6,12-16,18-21,24,25), on the preparation of the hexaborides of erbium, thulium, lutetium and scandium, investigations into the preparation of these hexaborides were reopened with the intent of obtaining information about the products--precise lattice parameters and thermodynamic stability data.

Another section of the rare earth boride review by Eick predicts that in those cases where rare earth tetraborides are less stable than the corresponding hexaboride, a sufficiently high temperature should cause the occurrence of the disproportionation reaction

$$3MB_4(s) \rightleftharpoons 2MB_6(s) + M(g).$$

Such a tetraboride is formed by samarium--indeed, the preparation of samarium tetraboride rather than the more stable hexaboride constituted a minor project in itself--and since the free energy change accompanying this reaction should reflect the relative stabilities of the two borides, experiments were planned which would allow the determination of the equilibrium vapor pressure of gaseous samarium over a mixture of the two borides at various temperatures, and, from this equilibrium vapor pressure data, calculation of the standard thermodynamic quantities of enthalpy and entropy for the reaction. For these vapor pressure measurements, the Knudsen effusion method was chosen as being most adaptable to the system.

II. THEORETICAL CONSIDERATIONS

A. Thermodynamics

Because of the natural limitations on physical systems at equilibrium summarized in the familiar phase rule, $F = C-P + 2$, where F is the number of degrees of freedom, P the number of phases present and C is the minimum number of components necessary to describe the system. A system (such as that under study) containing three phases (vapor, hexaboride and tetraboride) and two components (samarium and boron) must have a unique equilibrium vapor pressure at any given temperature.

By recording the equilibrium vapor pressure at various temperatures, and calling upon other thermodynamic data, the value for the standard free energy change accompanying the conversion of tetraboride into hexaboride and samarium vapor can be obtained.

1. Relationships Arising from the Second Law of Thermodynamics

For the reaction

$$3\ SmB_{4(s)} = 2\ SmB_{6(s)} + Sm_{(g)} \qquad (1)$$

at temperature T^{o} K.,

$$\Delta G^{o}_{T} = \Delta H^{o}_{T} - T\ \Delta S^{o}_{T} = -RT\ln K_{eq} = -RT\ln P_{Sm(g)} \qquad (2)$$

where K_{eq} is the equilibrium constant--for this reaction the vapor pressure of samarium.

For the case where the change in the constant pressure heat capacity is constant, the expressions for ΔH^{o}_{T} and ΔS^{o}_{T} are given by equations (3) and (4) respectively.

$$\Delta H_T^0 = \Delta H_\theta^0 + \int_\theta^T \Delta Cp\,dT = \Delta H_\theta^0 + \Delta Cp\ (T - \theta) \qquad (3)$$

$$\Delta S_T^0 = \Delta S_\theta^0 + \int_\theta^T \Delta Cp\ \frac{1}{T}\ dT = \Delta S_\theta^0 + \Delta Cp \ln\left(\frac{T}{\theta}\right) \qquad (4)$$

θ is a reference temperature; in this work 298.16°K. will be used.

Combination of the above equations (2), (3) and (4) leads to

$$-RT\ln K_{eq} = -RT\ln P_{Sm(g)} = \Delta G_T^0 = \Delta H_\theta^0 + \Delta Cp(T - \theta) - T\Delta S_\theta^0 - T\Delta Cp \ln\left(\frac{T}{\theta}\right). \qquad (5)$$

If the value of ΔCp should be so small as to be negligible, equation (5) simplifies to

$$-RT\ln P_{Sm(g)} = \Delta H_\theta^0 - T\Delta S_\theta^0 \qquad (6)$$

and

$$\log P_{Sm(g)} = \frac{-\Delta H_\theta^0}{2.303RT} + \frac{\Delta S_\theta^0}{2.303R} \qquad (7)$$

where R is the molar gas constant and the number 2.303 arises from the conversion of natural to base 10 logarithms. From equation (7) it can be seen that numerical values of ΔH_θ^0 and ΔS_θ^0 may be obtained from the slope and intercept respectively of an equation in which $\log P_{Sm(g)}$ is a function of 1/T.

2. Estimation of Heat Capacity Change

The method used to estimate the value of ΔCp for the reaction under study first assumes that, at high temperatures, the ΔCv (which is further assumed to approximate ΔCp) amounts to 3R (R is the gas constant) for each atom in a solid compound (32) (hence 21R for samarium hexaboride and 15R for samarium tetraboride). Treating samarium as an ideal, monatomic gas with no electronic contribution to the heat capacity results in a value of 5/2 R for its heat capacity. These assumptions

lead to an estimated minimum of -1/2 cal./deg. for the heat capacity change for the reaction. (An electronic contribution to the heat capacity of samarium gas would result in the algebraic addition of a positive term to the estimated minimum.)

If the absolute value of ΔCp is less than 1.0 cal./deg., the maximum values for $\Delta Cp(T-\theta)$ and $\Delta Cp\ \ln(T/\theta)$ are 2.0 kilocalories and 4.25 calories respectively.

Should ΔCp equal zero, the plot of $\log_{10}P_{Sm(g)}$ versus $1/T$ must be a straight line; the observation of such a straight line relationship would provide eloquent testimony that the true value for ΔCp is very close to zero in the temperature range studied.

3. Third Law Determination of Standard Enthalpy Change

Because of its use of absolute entropies and heat capacities, this method is fundamentally related to the Third Law of Thermodynamics. In order to corroborate the results from the treatment of data by the Second Law method, it is useful to obtain a value for the standard enthalpy change by employing the Third Law method since it is relatively insensitive to errors in temperature measurements.

The Third Law method makes use of the free energy function (hereafter abbreviated fef) defined by

$$\text{fef} = \left(\frac{G_T^0 - H_\theta^0}{T}\right) = \left(\frac{H_T^0 - H_\theta^0}{T}\right) - S_T^0 . \qquad (8)$$

Tabulations of free energy functions usually adopt 298.16°K. as a reference temperature leading to

$$\left(\frac{G_T^0 - H_{298}^0}{T}\right) = \left(\frac{H_T^0 - H_{298}^0}{T}\right) - S_T^0 . \qquad (9)$$

which is related to the free energy function at $0^{o}K.$ by the relation

$$\frac{G_T^o - H_{298}^o}{T} = \frac{G_T^o - H_o^o}{T} - \frac{H_{298}^o - H_o^o}{T} . \qquad (10)$$

For a reaction

$$\Delta fef = \sum_{\text{products}} \frac{G_T^o - H_{298}^o}{T} - \sum_{\text{reactants}} \frac{G_T^o - H_{298}^o}{T} = \frac{\Delta G_T^o}{T} - \frac{\Delta H_{298}^o}{T} \qquad (11)$$

and, making substitution for ΔG_T^o from equation (2) gives

$$\Delta fef = - R \ln P_{Sm} - \frac{\Delta H_{298}^o}{T} \qquad (12)$$

which rearranges into

$$\Delta H_{298}^o = -T \Delta fef - RT \ln P_{Sm} \qquad (13)$$

or

$$\Delta H_{298}^o = - T[\Delta(\frac{G_T^o - H_{298}^o}{T})] - 2.303 RT \log P_{Sm}. \qquad (14)$$

It can be seen from equation (14) that an independent value for the standard enthalpy change for a reaction may be calculated from each pair of pressure and temperature measurements provided that the free energy functions are available. In the absence of tabulations of the free energy function, the fef for a substance can be calculated from heat capacities or from spectroscopic data on gases. In those cases where no actual spectroscopic or heat capacity data of any sort are available, estimates must be made; even so, the caluclated standard enthalpy change is still a very useful check on the values obtained via calculations based on the Second Law treatment of the vapor pressure data.

B. The Knudsen Effusion Method

The Knudsen effusion method of determining equilibrium vapor pressures within a container by measuring the number of molecules effusing through a small orifice of known area in a thin wall of the container is now well established. In 1909, Knudsen first showed that the number of molecules passing through an orifice of a container in unit time is the same as the number of molecules which strike a section of the wall having an area equal to that of the orifice, so long as the wall is very thin and the vapor phase within the container is behaving as an ideal gas (37). Therefore, measurement of the number of molecules effusing through a small orifice in a cell allows the determination of the pressure within the container.

1. The Knudsen Effusion Equation

The number of molecules striking a unit area of a container wall, Z_e, is $n\bar{c}/4$ per unit time, where n is the density of the gas in molecules per unit volume and $\bar{c}$ is the average molecular speed. Since $n = N/V$, $N = R/k$ and $V = RT/P$, we may write

$$Z_e = 1/4\ (P\bar{c}/kT) \qquad (15)$$

where N is Avagadro's number, k is the Boltzman Constant, V the volume, P the pressure and T the absolute temperature.

The net rate of transfer of molecules out of the container is simply the number of molecules effusing per unit time, which is proportional to the internal pressure, less the number returning which is proportional to the external pressure of the species. Hence the effective effusion rate is

$$Z_e = 1/4 \left(\frac{P_1\bar{c}}{kT} - \frac{P_2\bar{c}}{kT}\right) \tag{16}$$

where P_1 is the internal equilibrium pressure and P_2 is the external partial pressure of the species. If P_2 is zero or $P_1 >> P_2$, equation (16) becomes

$$Z_e = 1/4 \frac{P_1\bar{c}}{kT} . \tag{17}$$

Making use of the Maxwellian velocity relationship

$$\bar{c} = \left(\frac{8RT}{\pi M}\right)^{1/2} \tag{18}$$

and multiplying both sides of equation (17) by M/N where M is the molecular weight of the effusing species leads to

$$Z_e\, M/N = \frac{M}{N} \frac{P}{4kT}\left(\frac{8RT}{\pi M}\right)^{1/2} = m \tag{19}$$

and

$$P = m \left(\frac{2\pi RT}{M}\right)^{1/2} = \frac{W}{S_0 t} \left(\frac{2\pi RT}{M}\right)^{1/2} \tag{20}$$

where R, the gas constant, is expressed in ergs/deg.-mole, m is the rate of mass effusion in g/cm^2-sec., and W is the weight of material effused through an orifice of area S_0 cm^2 during time t sec. Equation (20) is the basic Knudsen equation.

2. The Cosine Law Relationship

Although it is possible to determine the total number of grams of material effused from a cell by determining weight loss or by collecting the total effusate material, neither of these methods is universally applicable. The determination of weight loss is insufficiently accurate to measure extremely low pressures involved in some systems and requires

large samples. Total collection of an effusate is sometimes desirable; it is experimentally cumbersome and often unnecessary.

It has been shown (37,38) that the geometric distribution of effusate molecules escaping from an ideal, "knife-edged" orifice is governed by the cosine law represented by

$$dZ = Z_e(1/\pi)dS_0 \cos\Theta \, d\omega \, dt \qquad (21)$$

which indicates that the number of molecules escaping from the orifice, dZ, passing through an element of area dS_0 and through a conical section of elementary solid angle $d\omega$ oriented at angle Θ from the normal to the orifice plane (Fig. 5) is a function of the time, t, and the total effusion rate, Z_e.

Integration of equation (21) for which the reader is referred to the work of Carlson (38) indicates that the rate of molecular flux through an area unit located on the surface of a large sphere tangent to the orifice plane is everywhere equal. For this reason, the fraction of effusate striking a target located above an effusing orifice can be calculated so long as the distance from orifice to target and the orientation of the target are known. Hence, if a circular target of radius r is coaxial to the orifice at a distance d, the pressure P within a cell is related (37,38) to the number of moles, A, striking the target according to the equation

$$P = \frac{A}{S_0 t}(2\pi MRT)^{1/2}\left(\frac{r^2 + d^2}{r^2}\right) \qquad (22)$$

or, when S_0, t, and T are expressed in units of square centimeters, seconds and degrees Kelvin respectively, the pressure in atmospheres,

$$P = 0.022557 \frac{A}{S_0 t}\sqrt{TM}\left(\frac{r^2 + d^2}{r^2}\right). \qquad (23)$$

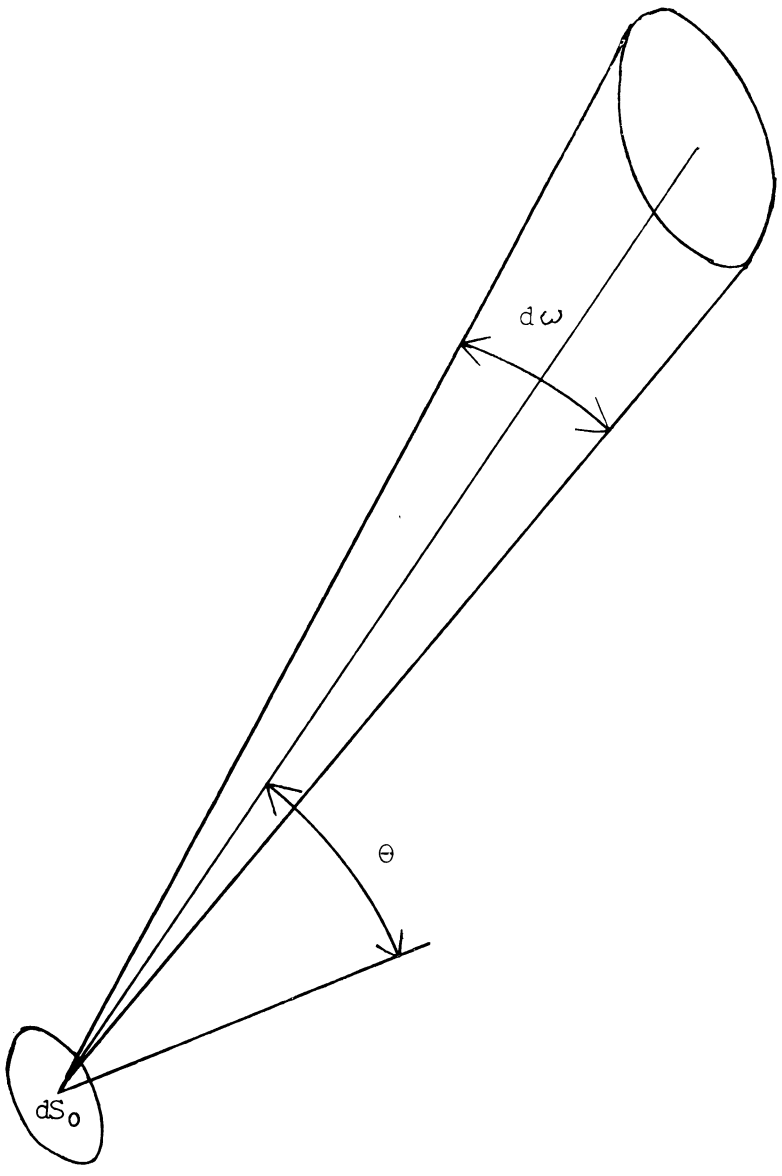

Figure 5. An element of a solid angle through which a gaseous particle effuses.

3. Limitations and Restrictions in the Knudsen Effusion Method

a. Equilibrium Vapor Pressure and the Vaporization Coefficient

The Knudsen method requires that the amount of material escaping through the effusion orifice have no significant effect on the equilibrium vapor pressure within the cell.

The vapor pressure of the evaporating species within an effusion cell where the rate of departure of particles from the solid phase is not sufficiently great to compensate for the loss from the vapor phase via effusion--hence to maintain equilibrium--is dependent upon the rate of evaporation of the effusing species from the surface of the solid (37,39). In these cases, the Knudsen effusion equation (23) must be further altered to include α, the vaporization coefficient which may be defined as the ratio of the actual number of particles leaving the solid phase to the number of particles leaving the solid phase under equilibrium conditions. The value of α will be seen to be unity when the evaporation rate of the particles is sufficient to maintain equilibrium in the effusion cell.

It is possible to detect those cases where the vaporization coefficient is not unity by comparing sets of pressure data obtained by using cells with two or more different orifice sizes. Smaller orifices restrict the material loss from the effusion cell to smaller absolute amounts.

In many cases, for a properly constructed effusion cell, no appreciable error results in assuming that the experimentally determined vapor pressure is the actual equilibrium vapor pressure (40). To fashion such

a cell, it is necessary that the size of the effusion orifice be very much smaller than the surface area of the solid phase from which evaporation is occurring.

b. Non-ideal Orifices

The Knudsen effusion equation (23) was developed with the requirement that the cell wall around the orifice be very thin; in practice this requirement means that the orifice must have a knife edge, i.e. the orifice must be a channel of infinitesimal length. Of course, it is experimentally impossible to fabricate an effusion cell meeting this requirement. In a theoretical study of the transmission of gaseous molecules through channels of finite length under molecular flow conditions, Clausing (41) found that the probability of transmission of such molecules through non-ideal orifices of certain geometric configurations is dependent indirectly both on the area of the orifice and the length of the orifice channel. Tabulations of numerical solutions to his equations for various dimensional shapes and sizes are available in the form of "Clausing factors" or transmission coefficients (42). Further discussions of this correction factor may be found in several reports (38,43-47).

c. Extraneous Chemical Reactions Within the Effusion Cell

Of course, no other reaction affecting the equilibrium must be taking place within the effusion cell. In general, this restriction requires that the products and reactants of the system under study must be analyzed to ascertain that the reaction taking place is accurately described by the chemical equation applied to the system.

Possible interaction of the reactants or products with the container must be considered, especially for high temperature systems, and even more especially for borides. Work performed in this laboratory by G. L. Galloway (48) demonstrated that molybdenum, tantalum and even tungsten, materials in common use for containing high temperature reaction mixtures, are unsuitable as containers for hot borides because of formation of molybdenum, tantalum or tungsten borides, respectively, accompanied by the release of the metal species of the contained boride.

d. Pressure Considerations in the Effusion Method

1. Molecular Flow Limitation: The Knudsen method requires that the gaseous species within the effusion cell not interfere with one another's motion during the effusion process. Knudsen himself reported (37) that at sufficiently high pressures within an effusion cell, hydrodynamic or fluid flow through the orifice occurs, such flow not conforming to the equations for molecular effusion and resulting in the escape of more material than under conditions of strict molecular flow; he prescribed the condition that the mean-free-path be 10 times greater than the orifice diameter to insure free molecular flow.

However, Carlson (38), who performed a detailed study of the problem found that deviation from the Knudsen flow condition took place when the ratio of mean-free-path to orifice diameter was unity. Furthermore, Habermann and Daane (47) measured vapor pressures of various rare earth metals at pressures up to 10^{-1} mm.Hg (corresponding to mean-free-path to orifice diameter ratios as low as 0.5). Wakefield (49) has measured the vapor pressure of holmium obtaining values as high as 10 mm.Hg without

noting deviations from the Knudsen flow condition. The conclusions of various workers concerning this complex problem are not in agreement and no satisfactory theoretical treatment which can be applied with confidence has appeared as yet.

Of the measurements reported in this thesis, fewer than one-tenth apply to cases where the mean-free-path to orifice diameter ratio is less than unity; and further, the value of the ratio is never less than 0.1. The collective findings of other workers together with the appearance of the data obtained in this work indicate that no significant complication has arisen due to excessively high pressures within the effusion cell.

2. Residual Pressure of the Vacuum System: Not only must the atmosphere surrounding the effusion cell have an effective pressure of zero for the effusing species as is required for equation (17), but the residual pressure of other gases must not be high enough to react with, scatter or otherwise interfere with the motion of the effusing vapor species toward the collection device.

e. Collection of Effusing Species

If the fraction of effusing material which strikes the target and also condenses there is not unity, it must be determined experimentally. The target must be kept as cool as possible to increase the probability of an impinging particle's "sticking". If condensation is not complete, "bouncing" experiments (described later) may be performed to determine the efficiency of collection by the targets.

In addition, the species being collected should not arrive at the target from any source or direction other than the effusion orifice. Error could arise if effusing species outside the collection angle were to reach the target by bouncing off the wall of the vacuum system and striking the target at the end of their secondary trajectory. The species being collected might also escape from the effusion cell through another hole in the cell, or by diffusion through the cell lid.

f. The Molecular Weight of the Effusing Species

From equation (23) it will be seen that the molecular weight of the effusing species must be known. The ideal method of verifying the molecular weight of the effusing species is by use of the mass spectrometer.

Mass specrometric data on the equilibrium distribution of molecular weights of the substance effusing from the cell can also be obtained from other work where the same substance is present in gaseous equilibrium. It is also possible to assume a molecular weight for the effusing species based on knowledge of the behavior of similar materials, or the same material at different temperatures, but such assumptions should be subjected to the closest scrutiny with actual measurement of the charge to mass ratio being reserved as a truly reliable method of obtaining the molecular weight.

g. Cell Temperature

The observed temperature, determined as precisely as possible, must be related directly to the internal temperature of the cell by a

determinable relationship. Gradients in the temperature within the cell generally are to be minimized and the avoidance of such gradients should be considered in the cell design.

The exponential dependence of pressure on temperature makes temperature determination the most critical of the physical measurements involved in this work.

III. EXPERIMENTAL METHODS

A. Synthesis of Borides

1. Starting Materials and Containers

Starting reactant and crucible materials for this research consisted of rare earth metals, rare earth sesquioxides, boron, boron carbide, graphite, boron nitride, zirconium diboride, molybdenum, and a molybdenum-tungsten alloy. Appendix I lists sources and purity levels for these materials.

Boron and the metal oxides were available in the form of powders. Metal powders were sometimes obtained by filing soft metals or by crushing hard metals in a diamond mortar. When in the form of powders, reaction mixtures, were mixed thoroughly in plastic containers using a Wig-L-Bug amalgamator (Crescent Dental Co., Chicago, Illinois). The mixed powders were pressed into pellets using a steel die under a hydraulic press (Carver Laboratory Press, Fred S. Carver, Inc., Summit, N. J.) employing a pressure of about 4,000 lbs./in.^{2}. When solid metals were used, it was not always practical to use powders so metal chunks and boron powder were simply placed together in a reaction vessel.

The ratios of boron to metal in reactant mixtures varied with experiment and were generally chosen to approach that ratio in the desired boride product with allowance being made when boron also reacted with oxygen in the reactant sample.

2. Induction Heating Experiments

The large majority of experiments were conducted in vacuum or an inert atmosphere in various crucibles heated directly or indirectly by the method of induction. The reaction containers were placed in a glass, Vycor and quartz system evacuated by means of a three-stage mercury diffusion pump backed by a Cenco Hyvac 14 fore pump. Unless an inert atmosphere was employed, the vacuum system pressure, which generally was in the range of 10^{-4} to 10^{-6} mm. Hg, was measured by means of a vacuum ionization gauge (Type Rg21A, Veeco Co., Hyde Park, N. Y.) attached to the system.

The actual choice of reaction container depended upon the intended purpose. Graphite crucibles were ideal in terms of availability, efficiency of heating and ease of machining. Boron nitride was easily machined and had the important advantage of showing no interaction with boride reaction mixtures. However, boron nitride is a non-conductor and therefore was heated indirectly by enclosing it in a graphite jacket. At temperaturesabove 1600°C., boron nitride becomes useless as a container because of material breakdown; the boron nitride begins to flake away from the surface of the material while fissures form in the bulk of the material itself.

Zirconium diboride was chosen as the primary container for the Knudsen effusion studies. Because of difficulties encountered in attempting to machine this material, crucibles were obtained commercially (Borolite Corporation, 3113 Forbes Ave., Pittsburgh 30, Pa.); only certain simple shapes were practically available. The zirconium diboride crucibles as supplied contained large amounts of binder material which

was driven from the crucibles by extended heating at temperatures up to 2100°C. until binder material ceased to condense on the walls of the vacuum line.

Zirconium diboride was tested as a boride reaction container by heating it at high temperatures (above 2100°C.) with a samarium hexaboride pellet inside. Although the boride migrated from the floor to the lid of the crucible, the deposit of the hexaboride came loose cleanly from the zirconium diboride lid after a subsequent heating at about 1500°C. In general, pellets of hexaboride or powder samples of tetraboride showed no tendency to bond to zirconium diboride even after being in contact with the crucible material for several hours at temperatures above 1500°C.

Molybdenum or molybdenum-tungsten alloys were used to fashion bombs when a closed reaction vessel was desired. Molybdenum and tungsten have been shown to interact with boride samples at high temperatures (48), but were still useable since the loss of a small amount of boron from the reaction mixture did not interfere with the formation of the desired product: the tetraboride.

3. Arc-melting Experiments

A number of samples of rare earth metals and boron pressed into pellets were fused under an argon atmosphere in an arc-melter equipped with a water-cooled, tungsten-tipped electrode and a water-cooled copper floor. An electric arc was struck between the sample and the tungsten-tipped electrode resulting in the rapid heating and melting of the sample. Once the sample was fused, the arc was broken or moved away from the sample which then almost instantaneously solidified. The sample was then flipped over and remelted to assure a homogeneous product.

4. Analysis of Reaction Products

All reaction products and some incompletely reacted mixtures were subjected to X-ray powder diffractometry analysis. This method may be expected to detect phases present to the extent of five percent or more in a mixture of phases. It was not always possible to identify all phases shown by X-ray methods to be present in products, but, within the limit of the method, it was frequently possible to ascertain the absence of phases of certain symmetries when the appropriate diffraction patterns were not observed.

Since many of the boride reaction products were mixtures of borides of different stoichiometries, or of boride and excess boron or metal, quantitative elemental analyses were unwarranted. The limitations of X-ray powder diffraction analysis made it possible that boride phases were present yet undetected in reaction products, but did not seriously hamper the interpretation of results. The absence of a particular phase, although not directly determined, could usually be concluded on the basis of phase-rule considerations and by observing the course of reactions by means of quenching reaction mixtures at various time intervals during the reaction process. Quenched reaction mixtures were subjected to X-ray powder diffraction analysis so that the course of a reaction could be followed.

A résumé of reaction mixtures, containers, temperatures, length of time at reaction temperature and products is given in Table I.

5. Product Boride Purification

Only in the case of samarium boride products prepared for use in

Table I. Reaction resume listing reactants, containers, temperatures, times, products and identifying X-ray photograph number.

Series	Run	Reactants	Crucible	Temp.	Time (hours)	Products	X-ray Photo.
I	A	Er + 4B	BN	1445		Starting material	A-892
	B			1550		ErB_4	A-893,894
	C			1500	2	ErB_4, ErB_{12}	A-895,896
	D		ZrB_2	1840	1	ErB_4	A-899
	E			2040	0.5	ErB_4	A-904
	F			2065	2	ErB_4	A-905
	G			2154	0.5	ErB_4	A-910
	H			2125	5	Pellet disappeared	
II	A	Er_2O_3 + 14B	BN	1000	0.5	Er_2O_3	A-906
	B			1410	1	ErB_4 , ErB_{12}	A-907,908
III	A	Er_2O_3 + 12B + 3C	BN	1100	1	Borocarbide? *	A-937
	B			1340	0.25	ErB_4	A-941
	C		ZrB_2	1490	1	ErB_4, ErB_{12}	A-947
IV	A	ErB_4	ZrB_2	2140	2	ErB_4	A-911
	B			2150	1	ErB_4, ErB_{12}, ZrB_2	A-912
V	A	Er_2O_3 + $3B_4C$		1600	24		
	B			1550	20	ErB_4,?	A-999
	C			1705	1	ErB_4	A-1003
VI	A	Er + 6B	Cu	Arc	Melt	ErB_4, ErB_{12}	A-997
VII	A	Er + 12B	Cu	Arc	Melt	ErB_4, ErB_{12}, ?	A-998
VIII	A	Tm + 6B	Cu	Arc	Melt	TmB_4, TmB_{12}	A-1000
IX	A	Tm + 12B	Cu	Arc	Melt	TmB_4, TmB_{12}	A-1001,1002
X	A	Lu_2O_3 + $3B_4C$	ZrB_2	1430	18	LuB_4, LuB_{12}, ?	A-1007
XI	A	Tm_2O_3 + $3B_4C$	ZrB_2	1530	9	TmB_4	A-1008
	B			1810	1	TmB_4, ?	A-1011

Table I. (Cont.)

Series	Run	Reactants	Crucible	Temp.	Time (hours)	Products	X-ray Photo.
XII	A	$Sc_2O_3 + 3B_4C$	ZrB_2	1520	2.5	Sc_2O_3, ScB_2	A-1012
	B			1700	0.2	Sc_2O_3, ScB_2	A-1013
	C			1730	5	Sc_2O_3, ScB_2	A-1014
	D			1810	3	Sc_2O_3, ScB_2	A-1019
XIII	A	$Ho_2O_3 + 3B_4C$	ZrB_2	1520	1.8	HoB_4, HoB_6, HoB_{12}	A-1024
	B			1730	2		
	C			1770	1	HoB_4, HoB_{12}, ?	A-1025
XIV	A	$Dy_2O_3 + 3B_4C$	ZrB_2	1680	8	DyB_4, DyB_{12}?, ?	A-1030
	B			1620	6.7		
	C			1570	2.2		
	D			1640	3.5	DyB_4, ?	A-1054
	E			1790	9.5	DyB_4	A-1056
XV	A	$Ho_2O_3 + 6B$	ZrB_2	1920	1		
	B			2200	3	HoB_4, ?	A-1064
	C			2400	0.5	Pellet disappeared	
XVI	A	$Ho_2O_3 + 15B$	ZrB_2	1350	0.5		
	B			1650	0.2		
	C			2090	0.1	HoB_4, HoB_6, HoB_{12}	A-1224
XVII	A	$Er_2O_3 + 15B$	ZrB_2	1490	0.5		
	B			1960	0.1	ErB_4, ErB_{12}	A-1229
XVIII	A	Tm + 2B	Cu	Arc	Melt	TmB_2, TmB_4	A-1259
XIX	A	Sm + 4B	Mo bomb	1500	3		
				1050	1		
				1500	0.3		
				900	4	SmB_4	A-1232

*A question mark immediately following a phase identification formula indicates that the identification of that phase in an X-ray powder photograph is not absolutely certain. A question mark separated from other formulae by a comma indicates the presence of an unidentified phase or phases.

effusion experiments were any attempts made to purify the samples. Finely ground tetraboride products were treated with distilled water and then with dilute hydrochloric acid to remove excess samarium metal, although the metal was never observed in X-ray powder photographs of final reaction products. The powdered samples were then rinsed with water several times to remove the acid, rinsed with acetone and dried at 110° C. in a drying oven.

B. Effusion Experiments

1. Apparatus

a. Vacuum Assembly

The vacuum system and effusion assembly used in the effusion experiments was designed for this purpose by Dr. Harry A. Eick and Mr. Robert E. Gebelt and had been employed previously by Dr. Richard A. Kent for the measurement of the vapor pressure of thorium in equilibrium with thorium dicarbide (50). The apparatus, which is shown schematically in Figure 6, includes a backed, three stage mercury diffusion pump, Vycor condenser, a support for the effusion crucible, an optical window and a device for presenting targets to the effusate from the cell. Below the target disc holder is a magnetically operated fused silica shutter for controlling exposure time. Discs were exposed to the effusion beam in succession, and, after being exposed, were ejected by means of a magnetically operated tungsten push-rod into a Pyrex receiver and storage chamber.

b. Effusion Cell

The effusion cell was designed to meet the requirements of inertness

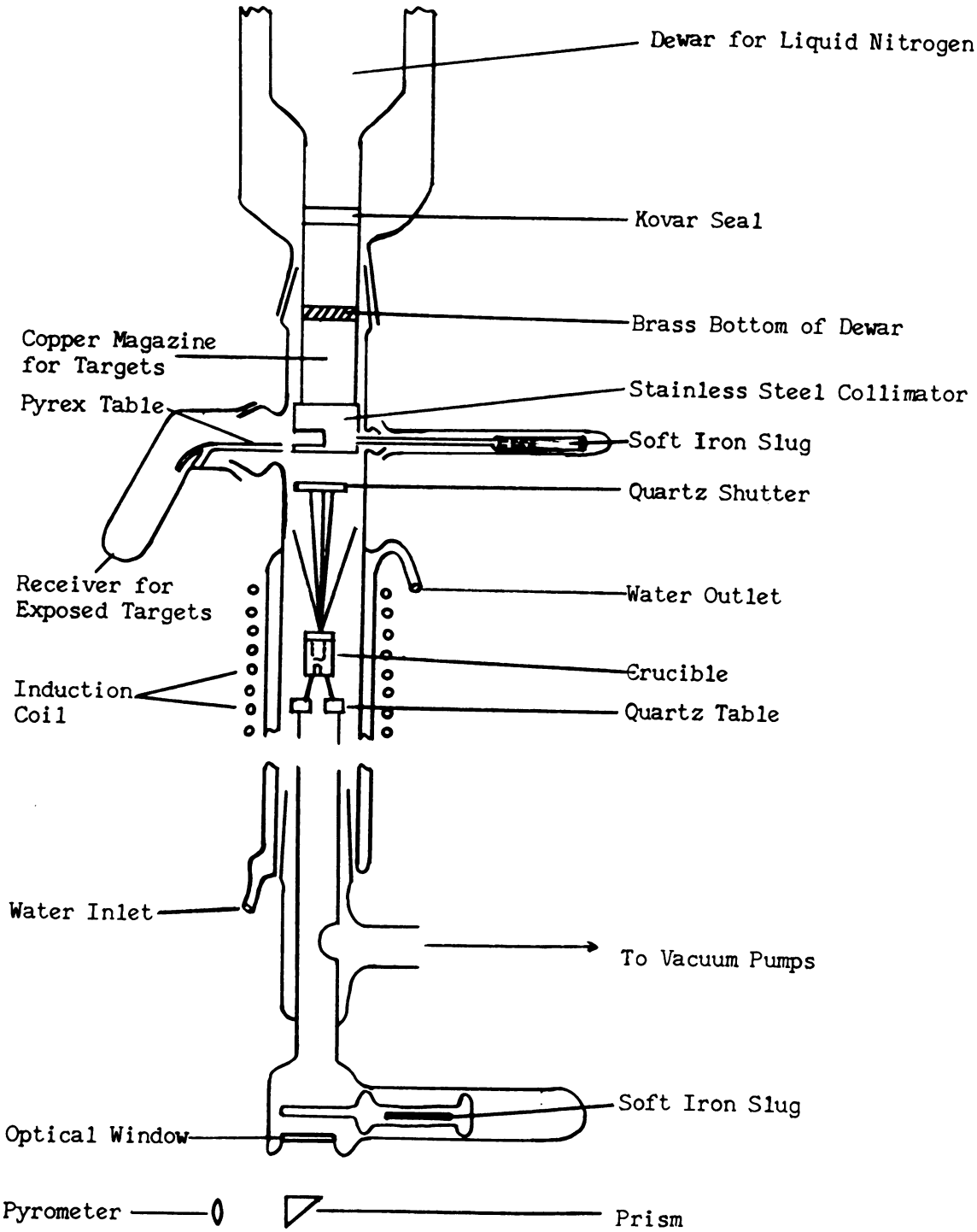

Figure 6 (50). Schematic diagram of vacuum system used for effusion experiments.

to hot boride mixtures and practicality of fashioning a suitable cell for effusion experiments.

Zirconium diboride was chosen as the primary container for the mixed samarium borides since preliminary experiments had shown it to be effectively inert to rare earth borides up to temperatures of 2000°C.

The bulk of the cell, which stood 38 mm. high, was fashioned from presintered molybdenum stock. Inside the molybdenum base, a zirconium diboride cup was positioned; it was denied contact with the molybdenum by means of symmetrically positioned tungsten pins, three in the floor and three in the wall of the cell.

The lid of the effusion cell, through which the effusion orifice had been drilled, was machined with a female taper; the base of the cell had a male taper to match that of the lid. Both sections of the cell and the zirconium diboride cup were outgassed prior to use. The molybdenum pieces were joined irreversibly when they were heated together for the first time.

The effusion cell is represented by Figure 7.

2. Measurement of Dimensions

The measurement of three linear dimensions is required for the Knudsen method calculations: the diameter of the effusion orifice of the crucible, the distance from the orifice to the target collimator and the diameter of the collimator. All linear parameters were measured several times each; an average value for each parameter was employed in the calculations.

Orifice diameter was measured before and after each effusion run using a microscope (Bausch and Lomb, Model SVB-73) equipped with a

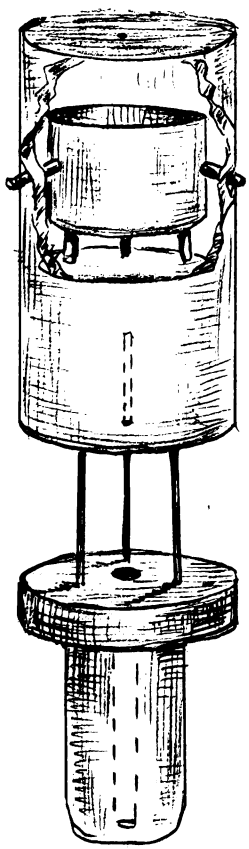

Figure 7. Pictorial representation of the Knudsen Effusion Cell.

vernier eye-piece calibrated such that one division on the vernier scale under high magnification (60X) measured 0.033 mm. The calibration of the eye-piece scale was verified by sighting on a gap between measuring posts of a precision micrometer.

After assembling the apparatus and evacuating it for at least half an hour so that the ground glass joints were firmly seated, the distance from the orifice to the collimator was measured with a cathetometer (Gaertner Scientific Company, Model No. M911, Serial No. 1585a). The scale could be read directly to 0.05 mm. by means of a vernier.

The position of the orifice of the effusion cell necessarily was determined by sighting through the double glass wall of the vacuum system and cooling jacket, but the position of the collimator lip was determined by sighting through the opening made by removing the shutter assembly.

The collimator diameter was measured with a vernier caliper which could be read to 0.004 inches. Appendix II lists tabulated values determined for the linear measurements pertaining to each effusion run.

3. Exposure Procedure

The evacuation of the effusion assembly always was begun the night before an effusion run. During each effusion run, the collimator-holder assembly was cooled by the introduction of liquid nitrogen into the Dewar-type container to which the collimator assembly was attached.

Before the first disc was exposed to effusate, the temperature of the cell was raised higher than the temperature desired for the exposure (except for the first run). Generally, a pressure rise was observed

when the cell was first heated; the cell was maintained at the higher temperature until the pressure of the system had receded to a value less than 1×10^{-5} mm. of mercury. The high pressures initially observed upon heating the effusion cell are ascribed to an outgassing process of the cell which was exposed to the air between runs.

When the system pressure had decreased sufficiently, the potential applied to the induction coil was adjusted to achieve a temperature within a few degrees of that projected for the exposure. The temperature was read at intervals of a few minutes until it appeared constant within two degrees; the shutter was then moved aside beginning the exposure of a disc.

The length of exposure time was chosen to produce a manageable deposit of samarium on the target disc, insofar as could be predicted. The time of each exposure was measured using a current frequency dependent timer (Lab-Chron, Labline, Inc., Chicago, Ill.) which recorded elapsed time to the nearest one-hundredth of a minute. The co-ordinated operation of the timer switch and shutter on the effusion assembly was performed manually.

Approximate temperatures for the individual exposures were planned in advance such that high temperatures were achieved during the middle of a series of exposures; hence lower temperatures were involved both before and after the high temperatures. This provided a check for reproducibility and a means of detection of such complications as surface depletion of samarium and dependence of the vapor pressure of samarium on the rate of diffusion of samarium to the surface of the sample.

4. Collection Efficiency; "Bouncing" Experiments

Pairs of discs, one above the other, were exposed to the effusing molecular beam of samarium. The lower disc in each pair was protected from the primary samarium molecular beam by a 0.127 mm. thick platinum disc situated below it. A small hole drilled in the lower quartz disc and a slightly smaller hole punched in the platinum disc (1.566 and 1.546 mm. for each platinum disc respectively) allowed some of the effusate to pass through, striking the second disc positioned directly above.

It is possible that some of the "reflected" atoms would escape to the side rather than strike the lower disc. This effect would be greatest when the cosine law for reflection was obeyed and then, because of the small distance between the two collectors, approximately 1.4% would fail to strike the lower disc. It is also possible that some impinging samarium atoms would strike the upper disc and reflect directly in the opposite direction passing back through the hole in the platinum disc through which they came previously.

Based on the assumptions that all samarium detected on the lower disc first had reflected from the upper disc (the primary beam would have had to penetrate the 0.127 mm. platinum) and that all the samarium which failed to "stick" to the upper disc was collected by the lower disc, an efficiency of collection was determined. Not enough individual "bouncing" experiments were performed to define a temperature dependence in the collection efficiency so an average value was used in all calculations. (See Appendix III).

C. Temperature Measurement

Temperatures were determined by means of disappearing filament optical pyrometers (Leeds and Northrup, Serial Nos. 1524388 and 1572579) calibrated by the National Bureau of Standards. The effusion cell and many of the crucibles employed for preparative work were provided with a black-body hole (generally considered to be a small hole drilled ten times as deep as the diameter of the hole) into which the optical pyrometer could be sighted.

Temperature readings were corrected for the transmissivity of the interposed optical window-prism combination. These corrections were determined by measuring the temperature of a particular area of the filament of a tungsten band lamp, with and without the prism and window interposed. The transmissivity corrections were assumed to be constant over the temperature range involved and were calculated from

$$1/C = 1/T_0 - 1/T_T$$

where T_0 is the observed temperature in degrees Kelvin, T_T is the true temperature in degrees Kelvin and $1/C$ is the transmissivity correction for a window or prism.

A total transmissivity correction for a system was calculated from

$$1/C_t = 1/C_p + 1/C_w$$

where $1/C_t$ is a total transmissivity correction, the sum of the transmissivity correction for prism and window. Thus, the true temperature was calculated from the observed temperature as in the following equation:

$$1/T_T = 1/T_0 - 1/C_t.$$

When the temperature of a container without a black-body hole was being determined, an emissivity constant was used to correct the apparent surface temperature to a black-body temperature. Since such containers were used only for preparative work where the temperature measurement was not critical, a graph was prepared by plotting observed temperature versus corrected temperature obtained by applying emissivity and transmission corrections. This graph was then used to convert observed temperatures into actual temperatures.

D. Quantitative Samarium Analyses

1. Preparation of Standards

Standard samarium solutions were prepared from two stock solutions containing known amounts of samarium nitrate. The stock solutions were prepared from weighed amounts of samarium sesquioxide, fired to constant weight in a muffle furnace, dissolved in a small volume of concentrated nitric acid and diluted to 250 ml. with demineralized water. Aliquots of the stock solutions were successively diluted to produce solutions containing very small concentrations of samarium ion as listed in Appendix IV.

Lambda pipettes were used to transfer small volumes of these dilute solutions onto quartz discs like those used for the effusion experiments. The discs with small volumes of the standard solutions were warmed with an infra-red heat lamp causing evaporation of the water and deposition of very small amounts of samarium on the discs. These quartz discs bearing their samarium deposits constituted the standards for the samarium analyses.

2. Neutron Activation of Samarium Samples

The discs from the effusion experiments, together with previously prepared standard discs and several blank discs, wrapped uniformly in aluminum foil, were exposed to a thermal neutron flux of at least 10^{12} neutrons/cm.^{2}-sec. in the CP-5 reactor at the Argonne National Laboratory (51). Exposure time for the discs from the first three runs was one week, for the last two runs, four days.

The irradiation resulted in an (n, γ) reaction of ^{152}Sm (26.7% abundance in naturally occurring samarium (52)) to ^{153}Sm which produces gamma activity of 104 Kev. energy with 47.1 h. half-life. Fortunately, the thermal neutron cross section for this reaction is very high, 140 barns, compared with the other reactions of samarium isotopes not resulting in stable masses so that no interfering gamma activity is produced in the neutron-activated samples. Appendix V presents data on samarium isotopes pertinent to neutron activation.

3. Identification of Species Present in Activated Samples

The gamma spectrum of an activated sample disc was recorded using the Baird Atomic gamma ray spectrometer (Model 250) with auxiliary recorder chart. The spectrum showed only the activity of ^{153}Sm as given by Crouthamel (53) and shown in Figure 8.

In addition, the half-life of the activity calculated from the decrease in activity with time for specific discs approximated the reported half-life of 47.1 hours.

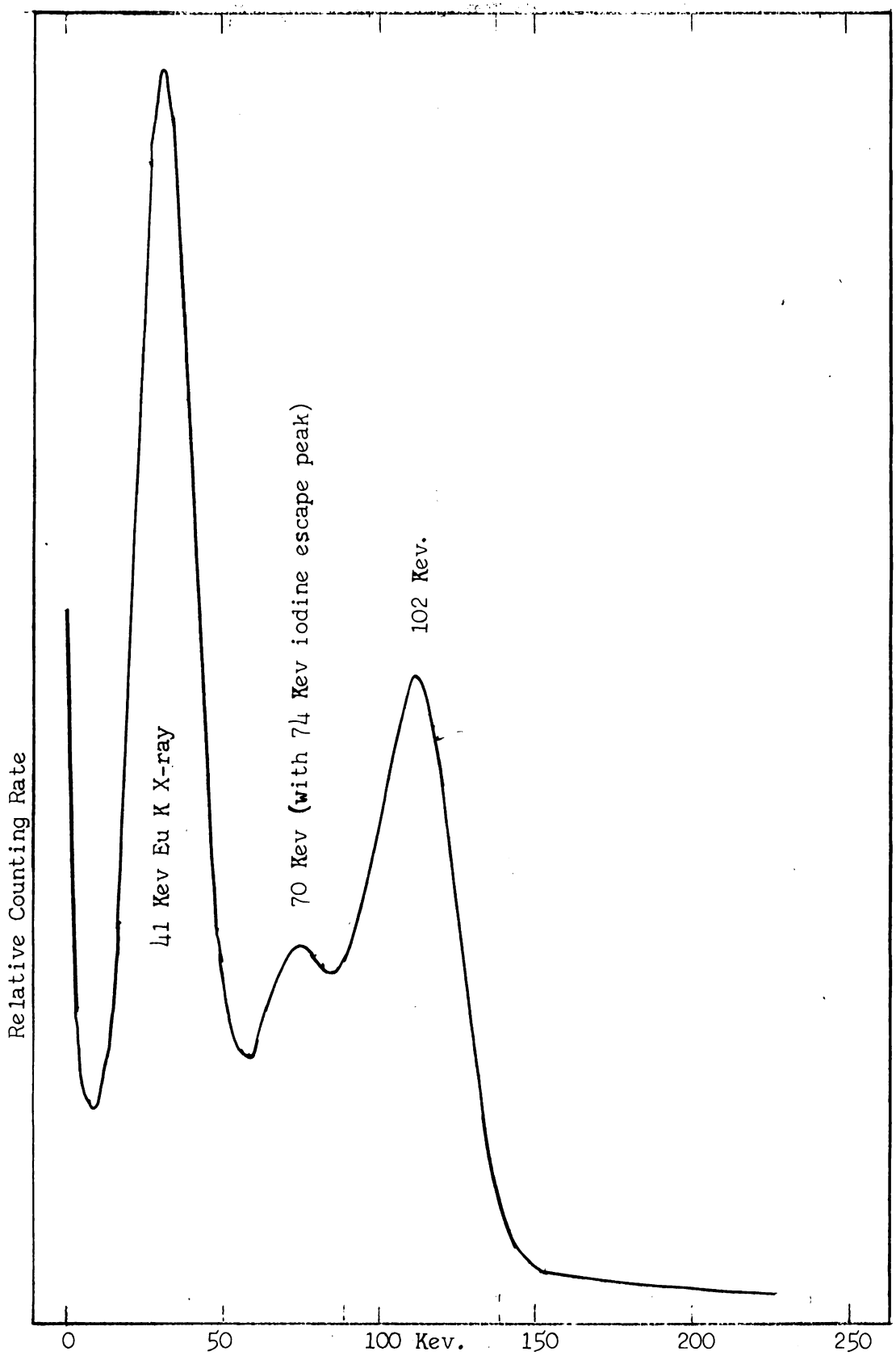

Figure 8. Gamma-ray spectrum of a neutron irradiated samarium-bearing quartz disc.

4. Counting of Activated Samples

The aluminum wrapper was removed from the samarium-bearing quartz discs which had been subjected to a thermal neutron flux and they were then rewrapped in "Saran" wrap in order to confine the samarium and protect the discs from direct contact with other materials.

The activities of the discs were determined in one of two differentiating scintillation counters (Baird Atomic amplifier-analyzer Model 250, Scalar Model 125; Hamner amplifier-analyzer Model N302, Scalar N221). A differentiating energy window of 100 Kev. centered on 102 Kev. energy was used. The sets of discs were counted several times in various orders until the least active samples gradually approached background activity rendering further counting purposeless.

It was hoped that, with the proper corrections for half-life of the activity and coincidence of detector excitation, the standard discs would show a linear relationship between the activity counted and the amount of samarium deposited on the discs. However, attempts at determining a coincidence correction factor were never satisfactory and, ultimately, non-linear curves were prepared for each series of counting of standards and unknowns. By reading values from the curve prepared from data on the standards, the activities of the unknowns were used to obtain values for the amount of samarium present.

The agreement between amounts of samarium on each disc determined by separate series of countings was not extremely good (Appendix VI). Values which were subject to the least chance of error (as judged by the appearance of various series of data) were averaged to obtain the number of moles of samarium on each unknown disc. This provided the required information for use in the Knudsen effusion equation.

Part of the problem encountered in evaluating the active samples arose because of the wide range of activities exhibited in both unknowns and standards. No single standard curve could accurately cover the whole range of activity and concentration of samarium.

E. Molecular Weight of Samarium Vapor Species

In order to determine the molecular weight of the effusing samarium species, samarium metal was heated in a molybdenum crucible, the cover of which was pierced by a small orifice. The vapor escaping from this orifice into a vacuum was directed into the ionization chamber of the Bendix Time-of-Flight mass spectrometer. The entire charge-to-mass ratio spectrum was scanned and projected on a fluoroscope. Special attentiveness was directed to those areas with charge/mass ratios corresponding to dimeric and oxide samarium species.

IV. RESULTS

A. Synthesis Experiments

1. Hexaborides

No success was achieved in obtaining hexaborides of erbium, thulium, lutetium or scandium (see Table I). X-ray diffraction data for a typical preparation, an erbium sesquioxide-boron carbide reaction product, is given in Table II.

These nominally failing attempts are worthy of report, however, in that similar results have been met by others (26) and that reported preparations of these hexaborides have not been substantiated well.

2. Samarium Tetraboride

The first preparation of samarium tetraboride uncontaminated by hexaboride was accomplished by heating samarium and boron together in a molybdenum alloy bomb sealed with a platinum gasket which method was indicated as most promising by previous work done in this laboratory by Galloway (48). This method took into account knowledge concerning boron behavior in various containers and the tendency of samarium to vaporize from its tetraboride leaving hexaboride behind.

3. Europium Tetraboride

Using an approach quite similar to that which led to the formation of samarium tetraboride, the preparation of europium tetraboride was attempted. However, the presence of such a phase in reaction products was never detected.

Table II. X-ray diffraction data for an erbium sesquioxide-boron carbide reaction product

$d_{obs.}$ (Å)	ErB_{12} $d_{calc.}$	ErB_{12} (hkl)	ErB_4 $d_{calc.}$	ErB_4 (hkl)	$d_{obs.}$ (Å)	ErB_{12} $d_{calc.}$	ErB_{12} (hkl)	ErB_4 $d_{calc.}$	ErB_4 (hkl)
5.019			5.000	110	1.670*	1.673	420	1.666	330
4.326	4.321	111			1.577			1.576	411
4.011			4.000	001	1.539			1.538	331
3.750	3.742	200			1.527	1.528	422		
3.538			3.536	200	1.490			1.490	312
3.161			3.162	210	1.440	1.440	333/511		
2.646	2.646	220	2.648	201	1.334			1.333	431
2.479			2.480	211				1.332	003
2.259	2.257	311			1.324	1.323	440		
2.236			2.236	310	1.312			1.313	520
2.161	2.160	222						1.310	511
2.121			2.120	221	1.302			1.301	412
2.000			1.999	002	1.280			1.280	332
1.952			1.951	311	1.265	1.265	531		
1.871	1.871	400			1.248	1.247	600	1.247	203
1.762			1.761	321	1.212			1.213	530
1.741			1.740	202	1.184	1.183	620		
1.714	1.716	331	1.715	410	1.161			1.160	531
1.689			1.689	212	1.142	1.141	533		

*Diffuse.

4. Thulium Diboride

Thulium diboride was prepared for the first time by arc-melting a pellet containing boron and thulium in a ratio of 2.0 (B/Tm). The preparation is not pure since a large amount of tetraboride is also formed. X-ray powder data obtained from the thulium boride reaction product are listed in Table III. Lattice parameters were calculated from the X-ray data without correction. They are a_0 = 3.25, Å and c_0 = 3.73 Å.

B. Knudsen Effusion Measurements

1. Comparison of Individual Runs

Considering a series of exposures of discs in succession at various temperatures without breaking vacuum as one run, it is apparent from the graph (Figure 9) showing the logarithm of samarium pressure versus reciprocal temperature (Appendix VII) that no significant difference or displacement was observed between the respective data resulting from various runs.

The last effusion run employed the same effusion cell with an enlarged orifice, again as a check to assure that the pressure measured was independent of the (small) orifice size and that the evaporization coefficient was essentially unity.

2. Collection Efficiency Determination

The results of the "bouncing" experiments listed in Appendix III indicate that an average of 94.5% of the impinging samarium atoms were retained on the target discs.

Table III. Observed d values for a thulium-boron reaction product with calculated d values for thulium borides

Estimated Intensity	Observed d value	Calculated* d values TmB_2	(hkl) TmB_2	Calculated** d values TmB_4	(hkl) TmB_4
30	3.943			3.976	001
40	3.719	3.731	001		
20	3.506			3.519	200
55	3.131			3.147	210
2	3.021			3.107	111
80	2.809	2.818	100		
50	2.632			2.635	201
75	2.461			2.468	211
99	2.245	2.249	101		
1	2.219			2.226	310
15	2.106			2.109	221
25	1.982			1.988	002
25	1.940			1.942	311
20	1.865	1.866	002		
1	1.850			1.846	112
1	1.748			1.752	321
10	1.729			1.731	202
25	1.706			1.707	410
20	1.679			1.681	212
15	1.659			1.659	330
55	1.625	1.627	110		
55	1.570			1.568	411
60	1.558	1.556	102		
35	1.533			1.531	331
50	1.493	1.491	111	1.483	312
40	1.411	1.409	200		
5	1.329			1.325	003
50	1.322	1.318	201		
5	1.308			1.304	511
45	1.301			1.295	412
30	1.280			1.274	332
20	1.248	1.244	003	1.240	203
50	1.233	1.226	112	1.222	213
20	1.214			1.207	530
10	1.179			1.173	600
35	1.163			1.156	531
40	1.146			1.149	432
40	1.127	1.125	202		

*a_0 = 3.25, c_0 = 3.73 Å. **a_0 = 7.071, c_0 = 3.997 Å

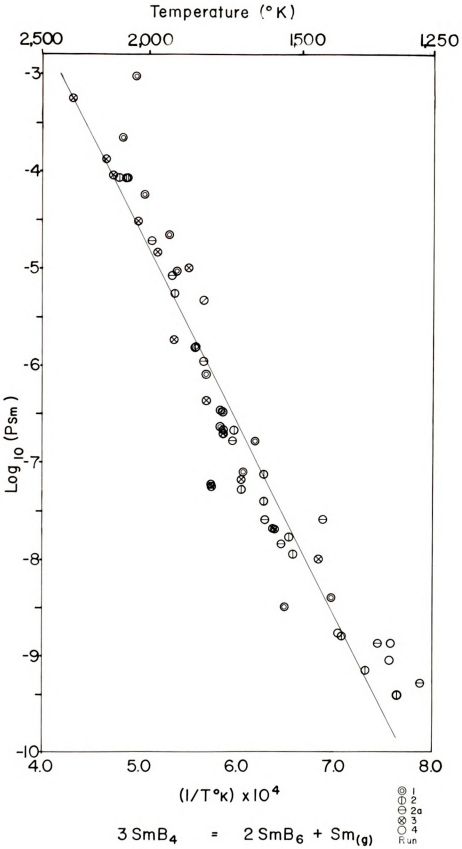

Figure 9. Graphical Representation of Knudsen effusion data.

3. Calculated Values for Enthalpy and Entropy Changes (Second Law)

The method of least squares was applied to the logarithm of pressure versus reciprocal temperature data to obtain the slope and intercept of the best straight line passing through the points. From the slope and intercept of the line were calculated the standard enthalpy and entropy changes for the reaction which results in the conversion of samarium tetraboride into samarium hexaboride and elemental samarium.

Four points obtained during various runs were rejected after visual inspection of a preliminary graph of the data. These points were initial points for the various series of exposures and showed pressures far too high to be consistent with the bulk of the data. Presumably, residual oxygen-containing gases react with the effusion cell contents to produce lower samarium oxides. These volatile oxides are collected on the quartz targets adding to the amount of samarium. As the residual gas pressure subsides this effect diminishes. With the exception of those four points, all points were given equal weight in calculating the least squares equation describing the data. For none of the points accepted was the distance to the least squares line greater than twice the standard deviation.

From the slope, a standard enthalpy change of 91.32 kilocalories with a standard deviation of 3.32 kilocalories was obtained. The intercept leads to values of 24.62 and 1.95 calories for the standard entropy change and its standard deviation respectively.

4. Calculated Values for Enthalpy Change (Third Law)

By estimating the fef of the borides to be the sum of the fef's of

the components, and employing the fef values for samarium given by Stull and Sinke (54), ΔH^{o}_{298} was calculated for each pressure-temperature point in the data. In spite of the gross scatter in the values calculated for the standard enthalpy change, no trend dependent upon temperature was observed in the data. All calculated standard enthalpy change values (with the exception of those for the four rejected points) were combined to obtain an average value of 93.93 kilocalories with a standard deviation of 2.01 kilocalories. The values for the standard enthalpy calculated by the Third Law method for each point are listed in Appendix VIII.

C. Determination of Molecular Weight of Effusing Species

Within the limits of detection (10^{-7} mm. Hg) and the temperature limit for the heating source of the mass spectrometer (1500°C), only monatomic samarium metal species were observed in the effusate escaping from a molybdenum cell containing metallic samarium.

V. CONCLUSIONS

A. Reports of Hexaborides of Erbium, Thulium, Lutetium and Scandium

With the exception of a report dating from 1932 (3) by von Neuman and Stackleberg, when pure samples of rare earths or their compounds were not available, all primary reports of erbium, thulium, lutetium and scandium hexaborides have arisen in the U.S.S.R., most often in the papers of G. V. Samsonov and co-workers. These reports are disturbing in that no success in preparing these hexaborides was achieved in this laboratory. A number of approaches were tried including experiments using carbon-containing reactants with the thought that the presence of carbon might stabilize a hexaboride phase. Ultimately, it was observed that products of reactions designed to lead to a boron-to-metal ratio of six often contained a mixture of borides: the tetraboride and the dodecaboride (Table II).

The details of the Russian preparative methods were not reported, but some X-ray powder crystallographic data were obtained indirectly by estimating diffraction angle values from a graphical representation of an X-ray powder photograph (13). These data proved to be subject to an interpretation different from that of the authors of the paper. In Table IV are presented the data of Neshpor and Samsonov with the interpretation of the researchers and the alternative interpretation of Sturgeon and Eick (55) which concludes that cubic hexaboride is absent.

Other preparative attempts have resulted in the formation of mixed tetra- and dodecaborides of lutetium: Przybylska, Reddoch and Ritter (26) have obtained results analogous to those reported here when they attempted

Table IV. Alternative interpretations of X-ray diffraction data for lutetium boride.

Neshpor and Samsonov(13)			Sturgeon and Eick (55)	
(hkl) LuB_6	(hkl) LuB_4	d (Å) obs.	d (Å) (calc.)* LuB_4	(hkl) LuB_4
100		3.94	3.96	001
110	210	3.14	3.15	210
	201	2.62	2.63	201
111		2.44	2.46	211
	310	2.24	2.23	310
200	221	2.08	2.11	221
210	320	1.93	1.95	320
	112	1.85	Probably Lu_2O_3	
211	022	1.73	1.73	202
	410	1.71	1.71	410
	212	1.68	1.68	212
	401	1.67	1.66	330
	420	1.57	1.58	411
	331	1.53	1.53	331
220	421	1.48	1.48	312
	430	1.43	1.41	430
221	510	1.41	1.39	322
	520	1.33	1.32	431/003
310	113	1.29	1.29	412
	332	1.28	1.27	332
311	123	1.25	1.25	203
	330	1.23	1.22	213
222	411	1.21	1.21	530
	610	1.18	1.16	531

*$a_0 = 7.04$, $c_0 = 3.96$ Å.

to prepare lutetium and scandium hexaborides. Instead of the cubic hexaborides which they sought for nuclear magnetic resonance investigations, they obtained mixtures of other borides.

My conclusion is that, until more detailed and satisfactory data are presented, the reports of the preparation of the hexaborides of lutetium, thulium, erbium and scandium must be discounted.

B. The Effect of Metallic Size on the Stability of the Cubic Hexaborides

In 1957, Muetterties (56) proposed size limitations on the metallic radii of metals for which metal borides could be formed, apparently on an empirical basis. His lower value (1.80 Å.) for hexaboride formation indicated that the heavy lanthanons (excluding ytterbium) should not form hexaborides. Such a limitation has been reported for the dodecaborides as well (9,23,27).

The preparation of cubic hexaborides for the rare earth metals becomes progressively more difficult as the metallic radius of the metal becomes smaller. The smallest metal for which a cubic hexaboride definitely has been prepared is holmium (metallic radius = 1.79 Å.) and this only in very small amounts (36). It appears that a limiting minimum metallic radius is reached at holmium among the rare earths indicating that cubic hexaborides of erbium, lutetium, thulium and scandium do not exist. Furthermore, it is likely that this minimum limitation is actually the result of a limiting minimum on the boron-boron distance which reaches 1.69 Å. in holmium hexaboride. No compounds containing smaller boron-boron single bonds of this type have been reported. Table V contains maximum and minimum boron-boron distances observed for the various types of rare earth borides.

Table V. Observed boron-boron distances in those types of borides exhibited by the rare earths.

Type		Maximum B-B (Å)	Metal	a_o (Å)	c_o(Å)	Minimum B-B (Å)	Metal	a_o (Å)	c_o(Å)
MB_2		1.91	Gd	3.31	3.94	1.71	Cr	2.969	3.066
MB_4	BI-BI	1.77	La	7.30	4.17	1.69	U	7.075	3.979
	BI-4 BIII	1.76				1.69			
	BII-BII	1.80				1.74			
	BII-2 BIII	1.80				1.75			
	BIII-2 BI	1.76				1.69			
	BIII-BII	1.80				1.75			
	BIII-2 BIII	1.81				1.75			
MB_6		1.78	Ba	4.268		1.69	Ho	4.096	
MB_{12}		1.769	Tb	7.505		1.746	Zr	7.408	

C. The Preparation of New Rare Earth Borides

Because the lattice parameters of the binary borides vary almost directly in proportion to either the metallic or ionic radii of the central or heavy metal and because the size of the metal atom is often the deciding factor for stability or instability, lattice parameters reported for compounds which do not conform to the pattern of other members of the same stoichiometric group of compounds are either suspect or indicate that the metal involved has more than one effective metallic or ionic radius.

Table VI presents the known binary borides of the rare earths together with their reported lattice parameters.

From the observation of such a table, it has been possible to prognosticate the preparation of additional rare earth borides. Such was true in the case of thulium diboride. However, such "gaps" have rapidly been filled in the past two years, and the likelihood of preparing new binary borides is rapidly being exhausted except in the case of the borides with very high boron contents which are not yet well characterized.

D. Samarium Tetraboride Stability

The qualitative fact that samarium tetraboride is unstable at high temperatures with respect to decomposition into hexaboride and excess metal now can be stated in quantitative terms. It is interesting that the large positive enthalpy for the reaction requires that, under one atmosphere of samarium vapor pressure, the temperature must be increased to about 3,500°C (actually above the reported melting point of 2,540°C (6)) before the negative entropy can overcome the positive heat resulting in the negative free energy change required for spontaneous reactions.

Table VI. Lattice parameters for known rare earth borides.

	Metallic radius (57)	MB_2		MB_4		MB_6	MB_{12}	ionic radius**
		a_0	c_0	a_0	c_0	a_0	a_0	
Sc	1.6545	3.146	3.517					0.68
Y	1.7780	3.298	3.843	7.111	4.017	4.113	7.500	0.88
La	1.8852			7.30	4.17	4.143		1.04
Ce	1.8248			7.205	4.090	4.141		1.02
Pr	1.8363			7.20	4.11	4.130		1.00
Nd	1.8290			7.219	4.102	4.126		.99
Pm								
Sm	1.8105	?*	?	7.174	4.070	4.133	?	0.97
Eu	1.994					4.178		0.96
Gd	1.810	3.31	3.94	7.144	4.048	4.108		0.94
Tb	1.8005	3.28	3.86	7.118	4.029	4.102	7.504	0.92
Dy	1.7952	3.285	3.835	7.101	4.017	4.098	7.501	0.91
Ho	1.7887	3.27	3.81	7.086	4.008	4.096	7.492	0.89
Er	1.7794	3.28	3.79	7.071	3.997		7.484	0.87
Tm	1.7688	3.254	3.732	7.05	3.99		7.476	0.86
Yb	1.9397			7.01	4.00	4.147	7.469	0.85
Lu	1.7516	3.246	3.704	7.00	3.94		7.464	0.84

*Said to exist (28) but no lattice parameter is reported.

**Trivalent ion.

This indicates that samarium tetraboride melts congruently under one atmosphere of samarium pressure.

E. The Problem of Europium Tetraboride

The preparation of europium tetraboride continues to elude workers in the rare earth boride area. The most rational approach to preparing such a boride is by means analogous to those used to prepare samarium tetraboride--by confining boron and excess europium in a bomb and heating at various temperatures for periods of time up to several weeks. The failure of this method seems inconsistent with the data obtained for the samarium tetraboride-hexaboride conversion.

One would not expect the standard entropy for the reaction of hexaboride plus excess europium to differ greatly from the values for samarium hexaboride so that the difference in stabilities of the respective tetraborides of samarium and europium must be related to a difference in standard enthalpy changes. The continuing failure to prepare europium tetraboride is puzzling.

VI. ERROR ANALYSIS

An analysis of random error for a representative disc exposure, exposure number six, run III, in the Knudsen effusion experiments shows that the greatest error arises in the determination of the number of moles of samarium on the disc. In Table VII are listed the standard deviations for all measured parameters involved in the calculation of the logarithm of the pressure of samarium at a temperature. Table VII also shows the value of the standard deviation for each parameter divided by the parameter value times 100 to obtain more easily comparable percentages.

It is felt that the standard deviation calculated for the area of the effusion orifice is misleadingly large since it was calculated on the basis of the assumption that the orifice was perfectly symmetrical which in fact it was not. This means that the scatter in the values determined for the radius is not due to random error, but rather to actual variances in the diameter of the orifice dependent upon which point of the perimeter was chosen as the end of the diameter. A large systematic error in the determination of the effusion orifice area for a single run should lead to displacement of its line on the graph describing the data from the line describing data from other runs. Within the limitations of the data, no such displacement was observed.

Some of the variation in observed temperature no doubt was truly random error encountered in matching apparent black-body temperature with that of the hot filament in the optical pyrometer. A standard deviation was estimated to be eight degrees for this type of error.

Table VII. Standard deviations of parameters measured for use in the Knudsen effusion equation.

	Parameter	Value of Parameter A	Standard Deviation B	$(\frac{100A}{B})$ %
S_0	Orifice area	7.524×10^{-3} cm.	8.70×10^{-5}	1.1
d	Cell to collimator distance	9.999 cm.	5.8×10^{-3}	0.6
r	Collimator radius	0.9535 cm.	8.4×10^{-4}	0.1
	Temperature	1743° K	8 (estimated)	0.46
	$(\text{Temperature})^{1/2}$	41.75	9.6×10^{-2}	0.3
t	Time	3600 sec.	negligible	---
A	Number of moles Sm	2.29×10^{-9}	6.1×10^{-10}	26.6

There is also systematic error in the temperature of approximately the same magnitude due to the limits of the calibration of the pyrometer.

However, an additional problem, of indeterminate extent, was introduced when voltage output from the low frequency generator to the induction coil used to heat the effusion crucible varied irregularly, uncontrollably and unpredictably—resulting in variations of the temperature, generally downward. Nonetheless, effusion runs wherein no such fluctuations were detected did not show appreciably greater precision.

Another complicating factor was the fact that higher than "equilibrium" pressure of samarium usually was observed for the first one or first few exposures in an effusion run. This may be attributable to the presence of oxygen which reacts to form a volatile samarium oxide (28) resulting in increased deposits of samarium on the target discs, an effect which diminishes as oxygen in the system is depleted. It may be attributable as well to interaction of small amounts of samarium tetraboride with the molybdenum cell since the boride had to be introduced into the cell through the effusion orifice itself, making it entirely possible that small amounts of the boride came into contact with the molybdenum instead of falling into the zirconium diboride cup. Thirdly, it is possible that not all elemental samarium was removed by treatment with dilute acid solution. In runs subsequent to the first, where the effusion cell was heated to high temperatures for some time before the exposure of the first disc was begun, this behavior was much less marked.

That the process of heating the effusion cell to a relatively high temperature to drive off excess samarium or other volatile samarium

species before beginning an effusion run did not result in samarium depletion of the tetraboride surface was indicated by the appearance of the sample after completion of the effusion runs. When the effusion cell was cut open, the sample was mostly the gray tetraboride with only a portion of the surface showing the blue of the hexaboride. The sample was still loosely powdered with no evidence of sintering.

The effect of varying the orifice size (i.e., no effect was observed in the pressures measured) indicates that the evaporation coefficient safely may be assumed to be unity.

In calculating the values for the standard enthalpy for the reaction studied, seventy-three points were used to calculate the slope of the least squares equation describing the points. The standard deviation in the slope calculated on the assumption that all points were randomly distributed around a mean, true value amounted to 3.6% of the value obtained for the slope. In the case of the intercept from which the standard entropy change is obtained, the standard deviation for the intercept amounted to 7.9% of the numerical value of the intercept, reflecting the lesser precision with which the intercept of the least squares equation is determined.

The high error in the pressure calculated from the Knudsen relationship is ascribable directly to the disappointingly large error in the assay for samarium by activation analysis. This error is not due to inadequacies of the activation process, but to limitations in the gamma-ray counting equipment available and its present state of precision in the thousands of counts per minute range.

The graph relating vapor pressure of samarium over a mixture of the tetra- and hexaborides to reciprocal temperature (Fig. 9) shows agreement

between runs, including the last run which was conducted with a different orifice size.

The values obtained from the Second and Third Law calculations agree within the limits of error.

Because of the nature of high temperature chemical systems and the many difficulties and limitations encountered in high temperature chemistry, such a large range of temperature and pressure measurements for one reaction is unusual. Some credit for this must be given to Dame Fortune since it was impossible to determine in advance what range could be studied practically.

VII. FUTURE RESEARCH

Because of the large cross section of ^{10}B for thermal neutrons, the otherwise desirable neutron diffraction experiments on borides are disallowed. Therefore, the only method of determining the exact boron positions in the rare earth borides is precise single crystal X-ray diffraction.

Using the thermodynamic data in this thesis and a measured free energy of formation of one of the samarium borides studied here, the calculation of the free energy of formation of the other would be possible.

Exploration of energy changes accompanying the conversion of other stoichiometry borides, not necessarily of samarium, will allow the quantitative description of other boride phase energy differences. Ultimately such data will lead to the delineation of phase diagrams which describe accurately rare earth boride systems.

The apparent consistency of electrical conductivity and Hall voltage data with the most recent theoretical discussions of the rare earth borides does not explain the fact that the hexaboride lattice parameters relate to the irregular metallic radii of the heavy metals while the lattice parameters of the dodecaborides and tetraborides reflect the different, regular trends visible in the radii of the triply charged metallic ions.

Since both the boranes and rare earth borides have been treated successfully using the same or similar theoretical approaches, efforts should be initiated in relating these two classes of compounds chemically.

Although it still appears reasonable that the tetraboride of europium should be preparable, no pertinent suggestions concerning a new experimental approach to its preparation come to mind.

Work in the area of high-temperature solid state materials will be benefitted increasingly by the accumulation of thermodynamic data concerning the substances involved--the values of heat capacities at high temperatures would be especially useful.

REFERENCES

1. Andrieux, L. Ann. Chim. (Paris) 12, 423 (1929).

2. Allard, G. Bull. Soc. Chim. France 51, 1213 (1932).

3. von Stackelberg, M. and F. Neumann. Z. Physik. Chem. (Leipzig) B19, 314, 1213 (1932).

4. Kiessling, R. Acta Chem. Scand. 4, 209 (1950).

5. Post, B., D. Moskowitz and F. W. Glaser. J. Am. Chem. Soc. 78, 1800 (1956).

6. Samsonov, G. V. Usp. Khim. 28, 189 (1959).

7. Aronsson, B. Arkiv Fysik 16, 379 (1960).

8. Eick, H. A. "Rare Earth Borides and Nitrides," Seminar at Lake Arrowhead, California, October, 1960, subsequently published in Rare Earth Research, E. V. Kleber, ed., The Macmillan Co., New York, 1961.

9. Post, B. "Refractory Binary Borides" Technical Rept. No. 6 Nonr 839 (12), NR 032-414, Polytechnic Institute of Brooklyn, Brooklyn, New York, 1963.

10. Zalkin, A. and D. H. Templeton. Acta Cryst. 6, 269 (1953).

11. Blum, P. and F. Bertaut. Acta Cryst. 7, 81 (1954).

12. Samsonov, G. V. and A. E. Grodshtein. Zh. Fiz. Khim. 30, 379 (1956).

13. Neshpor, V. S. and G. V. Samsonov. Dopovidi Akad. Nauk Ukr. RSR 1957, 478.

14. Zhuravlev, N. N. and A. A. Stepanova. Kristallografiya 3, 76 (1958).

15. Neshpor, V. S. and G. V. Samsonov. Zh. Fiz. Khim. 32, 1328 (1958).

16. Kudintseva, G. A., M. D. Polyakava, G. V. Samsonov and B. M. Tsarev. Fiz. Metal. i Metalloved. 6, 83 (1958).

17. Felten, E. J., I. Binder and P. Post. J. Am. Chem. Soc. 80, 3479 (1958).

18. Samsonov, G. V., N. N. Zhuravlev, Yu. B. Paderno and V. R. Melik-Adamyan. Kristallografiya 4, 538 (1959).

19. Samsonov, G. V., Yu. B. Paderno and T. I. Serebryakova. Kristallografiya 4, 542 (1959).

20. Tvorogov, N. N. Zh. Neorgan. Khim. 4, 1961 (1959).

21. Paderno, Yu. B. and G. V. Samsonov. Dokl. Akad. Nauk SSSR 137, 646 (1960).

22. La Placa, S. and B. Post, "Binary Dodecaborides", Technical Report No. 2, Nonr 839 (12), NR 032-414, Polytechnic Institute of Brooklyn, Brooklyn, New York, 1960.

23. La Placa, S., I. Binder and B. Post. J. Inorg. Nucl. Chem. 18, 113 (1961).

24. Paderno, Yu. B. and G. V. Samsonov. Zh. Strukt. Khim. 2, 213 (1961).

25. Vekshina, N. V. and L. Y. Markovskii. J. Appl. Chem. USSR English Transl. 34, 2067 (1961).

26. Przybylska, M., A. H. Reddoch and G. J. Ritter. J. Am. Chem. Soc. 85, 407 (1963).

27. La Placa, S., D. Noonan and B. Post. Acta Cryst. 16, 1182 (1963).

28. Nordine, P. Personal Communication.

29. Eberhardt, W. H., B. L. Crawford, Jr., and W. N. Lipscomb. J. Chem. Phys. 22, 985 (1954).

30. Longuet-Higgins, H. C. and M. de V. Roberts. Proc. Roy. Soc. (London), Ser. A 224, 336 (1954) and 230, 110 (1955).

31. Flodmark, S. Arkiv Fysik 9, 357 (1955); 14, 513 (1959) and 18, 49 (1960) and Svensk Kem. Tidskr. 70, 12 (1958).

32. Neshpor, V. S. and G. V. Samsonov. Zh. Neorgan. Khim. 4, 1966 (1959).

33. Lipscomb, W. N. and D. Britton. J. Chem. Phys. 33, 275 (1960).

34. Johnson, R. W. and A. H. Daane. J. Chem. Phys. 38, 425 (1963).

35. Kauer, E. Physics Letters 7, 171 (1963).

36. Eick, H. A. and P. W. Gilles. J. Am. Chem. Soc. 81, 5030 (1959).

37. Knudsen, M. Ann. Physik 28, 75 and 999, and 29, 179 (1909).

38. Carlson, K. D. "The Molecular and Viscous Effusion of Saturated Vapors," ANL-6156 (TID-4500, 15th Ed.), Argonne National Laboratory, Argonne, Ill. (1960).

39. Langmuir, I. Phys. Rev. 2, 329 (1913).

40. Ackermann, R. J. Argonne National Laboratory Report ANL-5482, Argonne National Laboratory, Argonne, Ill. (1955).

41. Clausing, P. Physica 9, 65 (1929); Z. Physik 66, 471 (1930) and Ann. Physik 12, 961 (1932).

42. Dushman, S. Scientific Foundations of Vacuum Technique, John Wiley and Sons, Inc., New York, 1949.

43. Freeman, R. D. and A. W. Searcy. J. Chem. Phys. 22, 1137 (1954).

44. DeMarcus, E. C. U. S. A. E. C. Report K1302, Parts I and II (1956); PartsIII and IV (1957).

45. Wahlbeck, P. G. Dissertation Abstr. 19, 2496 (1959).

46. Adams, J. Q. Dissertation Abstr. 21, 3643 (1961).

47. Habermann, C. E. and A. H. Daane. "Vapor Pressures of the Rare-Earth Metals", unpublished (submitted to J. Chem. Phys.)

48. Galloway, G. L. "Investigations into the Preparation and Decomposition of Samarium Tetraboride and Samarium Hexaboride", Ph.D. Thesis, Michigan State University, East Lansing, Michigan 1961.

49. Wakefield, G. F. "Vapor Pressure of Holmium Metal and Decomposition Pressure of Holmium Carbides", Ph.D. Thesis, Iowa State University of Science and Technology, Ames, Iowa 1957.

50. Kent, R. A. "The Vaporization and Thermodynamics of Thorium Dicarbide". Ph. D. Thesis, Michigan State University, East Lansing, Michigan 1963.

51. "Irradiation Services," Argonne National Laboratory, Argonne, Ill. 1959.

52. Seelmann-Eggebert, W., G. Pfennig, H. Münzel and G. Zundel. Chart of the Nuclides, 2nd ed., Bersbach and Sohn Verlag 32 Barer Strasse, München 34, Germany 1961.

53. Applied Gamma-Ray Spectrometry, C. E. Crouthamel, ed., Pergamon Press, New York 1960.

54. Thermodynamic Properties of the Elements, D. R. Stull and G. C. Sinke, American Chemical Society, Advances in Chemistry Series No. 18, Washington, D. C., 1956.

55. Sturgeon, G. D. and H. A. Eick. "Some Aspects of the Structure and Stability of the Cubic Hexaborides of the Lanthanons," to be published.

56. Muetterties, E. L. Z. Naturforsch. 12b, 411 (1957).

57. The Nature of the Chemical Bond, 3rd ed., L. Pauling, Cornell University Press, Ithaca, New York, 1960.

APPENDICES

APPENDIX I

SOURCE AND PURITY OF MATERIALS EMPLOYED

Source	Material	Purity
Michigan Chemical Corp. St. Louis, Michigan	Dy_2O_3	99.9%
	Lu_2O_3	99.9
	Tb_2O_3	99.9
	Y_2O_3	99.9
	Gd_2O_3	99.9
	Sm_2O_3	99.9
	Yb_2O_3	99.9
	Ho_2O_3	99.9
	Tm_2O_3	99.9
	Er_2O_3	99.9
	Eu_2O_3	99.8
	Eu	99
	Sm	99
	Er	99
	Tm	99
Heavy Minerals Corp. 4000 N. Hawthorne St. Chattanooga, Tenn.	Ho_2O_3	99.9
	Gd_2O_3	99.9
Research Chemicals Inc. Burbank, California	Sc_2O_3	99.9
U. S. Borax and Chemical Corp. Pacific Coast Borax Co. Division 630 Shatto Place, Los Angeles, Cal.	B	99.15
A. D. Mackay, Inc. 198 Broadway New York 38, N.Y.	B_4C	Unknown
Carborundum Latrobe, Pa.	BN	97.0 (2.4% oxide)
United Carbon Products Bay City, Michigan	Graphite	Better than spectroscopic
Borolite Corp. 3115 Forbes Ave. Pittsburgh 30, Pa.	ZrB_2	Unknown
Sylvania Electric Products, Inc. Chemical and Metal., Division Towanda, Pa.	Mo (effusion cell)	99.95
Climax Molybdenum Co. of Mich. Coldwater, Michigan	Mo (bomb)	> 99.9

APPENDIX II

COMPILATION OF CORRECTED LINEAR PARAMETERS FOR INDIVIDUAL EFFUSION RUNS

	S_0 orifice area($cm^2 \times 10^3$)	d orifice-target distance (cm.)	r target radius (cm.)	$\frac{r^2 + d^2}{r^2}$
Run I	7.421	10.037	0.9529	111.9
Run II	7.396	9.995	0.9532	111.0
Run IIa	7.498	10.001	0.9534	111.0
Run III	7.524	9.999	0.9535	110.1
Run IV	1.142	10.102	0.9550	112.9
"Bouncing" Experiments	1.142	10.199	0.07828 0.07730	16,970 17,410

APPENDIX III

DATA CONCERNING COLLECTION EFFICIENCY FOR KNUDSEN EFFUSION TARGET DISCS

First pair of target discs, exposed at 1788°K
upper disc (primary target) 53.1×10^{-10} mole Sm
lower disc (secondary target) 2.38×10^{-10} mole Sm

percent Sm collected on primary disc: 95.7%

Second pair of target discs, exposed at 2002°K
upper disc (primary target) 95.5×10^{-10} mole Sm
lower disc (secondary target) 7.53×10^{-10} mole Sm

percent Sm collected on primary disc: 92.7%

Average percent of Sm collected on primary discs: 94.2%

APPENDIX IV

DATA CONCERNING STANDARD SAMARIUM SOLUTIONS AND QUARTZ DISCS BEARING SAMARIUM DEPOSITS

Solution A: 0.54450 g Sm in 250 ml., 1.2492×10^{-2} M (Sm^{+3})

Solution B: 1.84275 g Sm in 250 ml., 4.2280×10^{-2} M (Sm^{+3})

Standard Quartz Discs

Run	Disc	Volume (λ)	Solution Concentration	Number of Moles of Sm ($\times 10^9$)
I	A	100	A	1,249
	B	10	B	422.8
	C	250	A/10	312.3
	D	300	B/100	126.8
	E	300	A/100	37.48
	F	300	B/1000	12.68
	H	400	A/1000	4.997
II + IIa	A	300	A/1000	3.745
	B	250	A/100	31.20
	C	200	A/10	249.6
	D	200	A	2,492.
	E	100	B	4,228.
	F	200	B/100	84.56
	G	300	B/1000	12.68
III + IV	A	200	B/10	845.6
	B	250	A/10	312.3
	C	100	B/100	42.28
	D	200	A/100	24.98
	E	100	A/100	12.49
	F	200	B/1000	8.456
	G	150	B/1000	2.114
	H	100	A/1000	1.249
	I	10	A/1000	0.1249

APPENDIX V

POSSIBLE (n, γ) REACTIONS FOR NATURALLY OCCURRING SAMARIUM ISOTOPES

Mass	Natural Occurrence	Cross Section (Barns)	Product Half-life	Product Decay Route (Mev)
144	3.09%	2	340 d	K-capture 0.66
147	14.97		stable	
148	11.24		stable	
149	13.83	40,800	stable	
150	7.44		~93 a	β^- 0.076 γ 0.02
152	26.72	140	47 h	β^- 0.70, 0.64, 0.80 γ 0.10, 0.07
154	22.71	5.5	24 m	β^- 1.65, 1.50 γ 0.11, 0.25

No active daughter species has a sufficiently short half-life to be detected in these experiments.

APPENDIX VI

SAMARIUM ASSAYS (Moles of Sm x 10^9)

Effusion Run I:

Disc	Counting Series 1	2	4	5	6a	6b	7a	7b	7c	8a	8b	9	8c	Average
1	0.72	1.7	1.65	1.03	1.01	1.42	-	-	-	-	-	-	-	1.255
2	0.65	2.2	1.95	0.71	0.80	1.26	-	-	0.94	-	0.08	-	0.88	1.05
3	0.76	2.4	1.96	1.40	1.30	1.81	-	-	1.85	-	-	-	-	1.64
4	1.53	3.64	4.17	4.60	2.4	3.15	-	-	3.9	-	-	-	-	3.34
5	2.95	4.66	8.67	9.60	6.0	6.67	-	-	9.24	-	-	-	-	6.83
6	1.70	1.5	3.47	2.53	2.0	2.66	-	-	2.22	-	-	-	2.24	2.29
7	0.85	1.27	2.56	1.53	-	2.19	-	-	1.9	-	-	-	5.0	2.19
8	0.465	0.86	1.68	0.60	-	-	-	-	1.07	-	-	-	0.93	0.934
9	3.76	2.8	13.8	11.85	10.5	10.46	-	8.0	-	-	15.2	-	-	10.03
10	-	-	47.5	-	85	-	52.2	43.1	-	67	51.2	70	-	60.75
11	2.5	-	8.18	6.88	5.75	6.52	-	-	6.11	-	-	-	-	5.99
12	0.48	-	1.93	0.80	0.75	1.13	-	-	1.2	-	-	-	1.17	1.066
13	0.22	-	1.05	0.044	0.15	0.48	-	-	0.5	-	-	-	1.13	0.511
14	0.34	-	1.36	0.383	0.625	0.9	-	-	1.02	-	-	-	1.39	0.860
15	-	-	112	-	195.	-	118.6	103.3	-	128	-	159	-	139.3
16	-	-	-	-	389	-	376	-	-	324	-	358	-	361.8
17	-	-	-	-	-	-	-	-	-	610	-	613	-	612
18	-	-	-	-	-	-	-	-	-	1252	-	1430	-	1341

APPENDIX VI (Continued)

Effusion Runs II and IIa

					Counting Series					
Disc	4	6x	6a	6b	6c	8a	8b	9a	9b	10	Average
1	-	151.4	-	150.0	-	-	136.9	236.8	220	220	185.8
2	-	38.8	32.0	35.0	-	43.6	46.5	31.0	31.0	-	36.84
3	0.34	0.2	-	-	-	-	-	-	-	-	0.373
4	0.11	0.07	-	-	-	-	-	-	-	-	0.267
5	3.05	1.6	-	-	1.34	-	4.9	-	-	-	2.87
6	0.90	0.4	-	-	-	-	-	-	-	-	0.813
7	0.285	0.26	-	-	-	-	-	-	-	-	0.355
8	0.71	2.95	-	-	-	1.1	-	-	-	-	1.435
9	0	0	-	-	-	-	-	-	-	-	0.0267
10	0	0	-	-	-	-	-	-	-	-	0.0367
11	0	0.002	-	-	-	-	-	-	-	-	0.054
12	0.48	0.21	-	-	-	-	-	-	-	-	0.467
13	-	1.00	-	-	0.6	-	-	-	-	-	0.80
14	-	14.7	13.3	14.6	11.3	15.6	15.9	-	16.1	-	14.8
15	1.05	0.44	-	-	-	1.2	-	-	-	-	0.933
16	3.80	1.94	-	-	-	2.5	2.1	-	-	-	2.18
17	-	238.3	-	218	-	-	190.0	380?	-	410.0	287.3
18	-	225.8	-	204	-	-	177.2	350?	-	325.0	258.5
21	-	2.61	-	-	3.25	4.6	4.0	-	-	-	3.61
22	0	0.002	-	-	-	-	-	-	-	-	0.034
23	0	0.002	-	-	-	0.2	-	-	-	-	0.061
24	1.11	0.50	-	-	-	1.5	-	-	-	-	1.12
25	0.44	0.27	-	-	-	-	-	-	-	-	0.456
26	0.54	0.50	-	-	-	0.8	-	-	-	-	0.807
27	-	1.95	-	-	1.6	3.4	3.2	-	-	-	2.538
28	-	16.0	11.1	12.5	9.85	12.5	11.5	-	15.8	-	12.75
29	-	54.2	50.25	51.1	-	40.43	47.2	65	71.0	-	54.17
30	-	67.6	62.6	50.25	-	48.00	51.6	70	75.4	-	60.78

APPENDIX VI (Continued)

Effusion Run III

Disc	Counting Series																
	1	2	4a	4b	5	6a	6b	6c	7	7a	7b	8a	8b	8c	9a	9a	Average
1	0.72	1.7	-	1.65	1.03	-	1.01	1.42	-	-	-	-	-	-	-	-	1.25
2	0.65	2.2	-	1.95	0.71	-	0.80	1.26	0.94	-	-	-	0.08	0.88	-	-	1.05
3	0.76	2.4	-	1.96	1.40	-	1.30	1.81	1.85	-	-	-	-	-	-	-	1.64
4	1.53	3.64	-	4.17	4.60	-	2.4	3.15	3.9	-	-	-	-	-	-	-	3.34
5	2.95	4.66	-	8.67	9.60	-	6.0	6.67	9.24	-	-	-	-	-	-	-	6.83
6	1.70	1.5	-	3.47	2.53	-	2.0	2.66	2.22	-	-	-	-	2.24	-	-	2.29
7	0.85	1.27	-	2.56	1.53	-	-	2.19	1.9	-	-	-	-	5.0	-	-	2.19
8	0.46	0.86	-	1.68	0.60	-	21.0	-	1.07	-	-	-	-	0.93	-	-	1.12
9	3.76	2.8	12.5	15.2	11.85	-	10.5	10.46	-	-	8.0	-	15.2	-	-	-	10.03
10	-	-	47.5	-	-	85	-	-	-	52.2	43.1	67	51.2	-	67	73	60
11	2.50	-	-	8.18	6.88	-	5.75	6.52	6.11	-	-	-	-	-	-	-	5.99
12	0.48	-	-	1.93	0.80	-	0.75	1.13	1.2	-	-	-	-	1.17	-	-	1.66
13	0.22	-	-	1.05	0.044	-	0.15	0.48	0.5	-	-	-	-	1.13	-	-	0.511
14	0.34	-	-	1.36	0.383	-	0.625	0.90	1.02	-	-	-	-	1.39	-	-	0.860
15	-	-	112	-	-	195	-	-	-	118.6	103.3	128	-	-	140	178.5	139.3
16	-	-	-	-	-	389	-	-	-	396	-	324	-	-	358	-	361.8
17	-	-	-	-	-	-	-	-	-	-	-	610	-	-	613	-	612
18	-	-	-	-	-	-	-	-	-	-	-	1252	-	-	1430	-	1341

APPENDIX VI (Continued)

Effusion Run IV

	Counting Series									
Disc	1a	1b	2a	$2b_1$	3b	3a	$2b_2$	5	6	Average
(2)1	15.2	-	17.5	18.3	-	18	-	-	-	17.2
(2)2	-	1.4	-	1.35	0.95	-	-	-	-	1.23
(2)3	-	1.125	-	1.4	1.65	-	-	-	-	1.39
(2)4	-	0.86	-	1.3	1.22	-	-	-	-	1.13
(2)5	13.0	11.65	10.935	11.0	8.62	8.0	-	-	-	10.5
(2)6	49.0	-	45.59	44.7	10.75	8.5	-	-	-	31.7
(2)7	72.7	-	66.67	81.5	-	65.0	-	-	-	71.5
(2)8	-	-	94.165	94.0	-	90.5	-	90	105	94.7
(3)9	-	-	-	-	-	-	-	580	440	510
(3)0	-	-	-	-	-	-	-	2700	2460	2580
(3)1	-	-	-	-	-	-	-	975	700	838
(3)2	-	-	-	-	-	-	-	3200	3169	3180
(3)3	-	-	-	-	-	-	-	4550	4200	4375
(3)4	-	-	-	-	-	-	-	1650	1210	1430
(3)5	-	-	-	-	-	-	-	952	705	828
(3)6	-	-	144.2	124.2	-	133.0	-	125	160	137.3
(3)7	71.5	-	70.0	70.0	-	65.0	-	-	-	69.1
(3)8	30.8	-	27.8	30.8	-	27.5	-	-	-	29.2
(4)1	2.4	3.5	2.26	2.75	2.425	-	3.31	-	-	2.38
(4)2	57.0	-	49.0	54.8	-	51.5	-	-	-	53.1
(4)3	8.6	8.325	7.51	6.5	6.9	6.0	8.85	-	-	7.53
(4)4	-	-	93.75	97.3	-	95.5	-	-	-	95.5

APPENDIX VII

LOG PRESSURE AND TEMPERATURE DATA FOR INDIVIDUAL EFFUSION EXPOSURES

Run I

Exposure	Corrected Temperature ^{o}K	Exposure Time (sec.)	- Logarithm of Calculated Pressure
1	1459	3601	7.231
2	1505	3601	7.301
3	1507	3600	7.107
4	1618	3600	6.783
5	1717	3601	6.459
6	1717	1801	6.633
7	1709	1200	6.477
8	1708	780	6.660
9	1793	1204	5.807
10	1859	1200	5.028
11	1760	1380	6.094
12	1649	2400	7.099
13	1541	2760	8.493
14	1436	3600	8.398
15	1886	1200	4.652
16	1980	1230	4.238
17	2014	1260	3.016
18	2071	1200	3.649

APPENDIX VII (Continued)

Runs II and IIa

Exposure	Corrected Temperature °K	Exposure Time (sec.)	- Logarithm of Calculated Pressure
1	2057	433.2	4.068
2	1866	1268	5.258
5	1676	2403	6.668
6	1594	3600	7.402
7	1522	5400	7.948
8	1595	3359	7.125
9	1309	10800	9.406
10	1367	8400	9.148
11	1404	5548	8.795
12	1531	4620	7.770
13	1655	2700	7.276
14	1796	1800	5.815
17	2049	660	4.063
18	2086	600	4.063
21	1275	6000	7.841
22	1270	7201	7.876
23	1344	7200	7.442
24	1454	7201	6.877
25	1550	5400	6.453
26	1591	5460	6.286
27	1681	2700	5.950
28	1769	2100	5.654
29	1875	1200	5.332
30	1951	600	5.125

APPENDIX VII (Continued)

Effusion Run III.

Exposure	Corrected Temperature $^{o}K.$	Exposure Time (sec.)	- Logarithm Calculated Pressure
1	1338	5400	7.490
2	1463	5460	7.997
3	1569	3660	7.688
4	1655	3600	7.178
5	1745	1800	7.224
6	1743	3600	7.242
7	1865	2400	5.733
8	2007	1920	4.512
9	2147	600	3.870
10	2315	300	3.240
11	2114	900	4.040
12	1967	1320	4.833
13	1818	1801	4.997
14	1768	300	5.326
15	1760	3000	6.360
16	1708	3660	6.699
17	1571	7200	7.681

APPENDIX VII (Continued)

Effusion Run IV.

Exposure	Corrected Temperature °K.	Exposure Time (sec.)	- Logarithm Calculated Pressure
(2)1	1263	14408	7.911
(2)2	1323	14400	9.047
(2)3	1320	10866	8.872
(2)4	1421	7200	8.765
(2)5	1518	7200	7.785
(2)6	1622	5400	7.127
(2)7	1716	1800	6.322
(2)8	1795	900	5.890
(2)9	1913	600	4.969
(3)0	2013	360	4.031
(3)1	2016	180	4.218
(3)2	2142	75	3.246
(3)3	2218	60	3.003
(3)4	2048	180	3.984
(3)5	1955	600	4.754
(3)6	1912	900	5.715
(3)7	1723	1800	6.336
(3)8	1630	2700	7.899
(4)2	1789	14700	7.158
(4)4	2003	3600	4.630

APPENDIX VIII

THIRD LAW STANDARD ENTHALPY CHANGE CALCULATED AT VARIOUS TEMPERATURES

Temperature °K.	ΔH°_{298} kcal.	Temperature °K.	ΔH°_{298} kcal.
1263	80.34	1717	96.83
1270	88.80	1717	98.19
1275	76.06	1743	104.50
1309	92.28	1745	104.46
1320	89.78	1760	87.46
1323	91.07	1760	98.39
1338	82.57	1768	90.44
1344	91.41	1769	95.58
1367	94.70	1789	112.98
1404	94.96	1793	95.65
1421	97.95	1795	88.86
1436	94.43	1796	95.86
1454	90.25	1818	90.12
1459	88.15	1859	92.05
1463	78.82	1865	98.28
1505	91.26	1866	94.33
1507	90.05	1875	93.10
1518	95.34	1886	89.92
1524	96.72	1912	100.61
1531	96.06	1913	93.55
1541	101.75	1951	94.06
1550	97.77	1956	92.61
1569	97.77	1967	92.59
1571	97.82	1980	88.48
1591	98.40	2007	91.51
1594	97.16	2013	87.22
1595	95.19	2014	77.87
1618	93.96	2015	89.00
1622	90.80	2049	87.50
1630	91.02	2049	88.20
1649	98.06	2057	88.36
1655	99.69	2071	84.71
1655	98.96	2088	88.83
1676	96.21	2114	86.98
1681	97.32	2142	81.83
1707	97.86	2147	88.04
1708	98.17	2218	80.50
1709	96.51	2315	84.37
1716	92.32		

CHEMISTRY LIBRARY

MICHIGAN STATE UNIVERSITY LIBRARIES
3 1293 03146 1530